A noncanonical role for the engulfment gene ELMO1 in neutrophils that promotes inflammatory arthritis

Engulfment gene *ELMO1* in neutrophils as a promoter of inflammatory arthritis

Sanja Arandjelovic[1*], Justin S.A. Perry[1], Christopher D. Lucas[1,2], Kristen K. Penberthy[1], Tae-Hyoun Kim[3], Ming Zhou[4], Dorian A Rosen[5], Tzu-Ying Chuang[5], Alexandra M. Bettina[1], Laura S. Shankman[1], Amanda H. Cohen[1], Alban Gaultier[5], Thomas P. Conrads[4], Minsoo Kim[3], Michael R. Elliott[3], and Kodi S. Ravichandran[1,5*]

[1]*University of Virginia, Center for Cell Clearance, Department of Microbiology, Immunology and Cancer Biology, Charlottesville, VA, USA.*

[2]*University of Edinburgh, Centre for Inflammation Research, Edinburgh, Scotland, UK.*

[3]*University of Rochester, David H. Smith Center for Vaccine Biology and Immunology, Department of Microbiology and Immunology, Rochester, NY, USA.*

[4]*Inova Schar Cancer Institute, Inova Center for Personalized Health, Fairfax, VA, USA.*

[5]*University of Virginia, Center for Brain Immunology and Glia, Department of Neuroscience, Charlottesville, VA, USA.*

[6]*Inflammation Research Centre, VIB, and the Department of Biomedical Molecular Biology, Ghent, Belgium*

* Corresponding Authors:

Kodi S. Ravichandran
Dept. of Microbiology, Immunology, and Cancer Biology
University of Virginia
Box 800734, Pinn Hall 7315
Charlottesville, VA 22908
Ph: 434-243-6093; Email: Ravi@virginia.edu

Sanja Arandjelovic
Dept. of Microbiology, Immunology, and Cancer Biology
University of Virginia
Box 800734, Pinn Hall 4067
Charlottesville, VA 22908
Ph: 434-982-2593; Email: sa2h@virginia.edu

SUMMARY

Rheumatoid arthritis is an inflammatory disease of the synovial joints that affects ~1% of the human population, with severe distress due to progressive joint inflammation and deformation. When addressing the links between specific components of the apoptotic cell clearance machinery and human disease, we noted a correlation between single nucleotide polymorphisms (SNPs) in *ELMO1, DOCK2,* and *RAC1* genes and rheumatoid arthritis. ELMO1 is a cytoplasmic adapter protein that associates with DOCK2 and RAC1 to promote cytoskeletal reorganization needed for apoptotic cell uptake by phagocytes. We initially hypothesized that, since ELMO1 is linked to apoptotic cell clearance, loss of ELMO1 would lead to increased inflammation in arthritis. Contrary to the accumulation of apoptotic cells and greater disease severity that we predicted, we observed significantly reduced joint inflammation in two models of arthritis in mice lacking ELMO1. Using genetic and cell biological approaches *in vivo* and *ex vivo,* we determined that ELMO1 deficiency significantly reduces neutrophil recruitment to inflamed joints, but does not result in general inhibition of inflammatory responses. Through proteomic analyses, we find that ELMO1 protein associates with cellular receptors that contribute to neutrophil function in arthritis, and regulates C5a and LTB4 receptor-mediated activation and early neutrophil recruitment to the joints. Neutrophil-specific transcriptomics show that ELMO1 modulates neutrophil-specific gene expression that includes genes with known linkages to human arthritis. Finally, neutrophils from the peripheral blood of human donors that carry the SNP in *ELMO1* associated with arthritis display increased migratory capacity, whereas *ELMO1* knockdown reduces human neutrophil migration to LTB4. These data identify key 'non-canonical' roles for engulfment machinery components in arthritis, and ELMO1 as an important regulator of specific neutrophil receptors and signaling linked to arthritis.

INTRODUCTION

Rheumatoid arthritis (RA), which affects millions of people worldwide with a huge personal 'quality of life' cost as well as a significant economic cost, is characterized by chronic joint inflammation and progressive destruction of the bone and cartilage, with debilitating consequences [1]. In human RA and mouse models of arthritis, leukocyte influx into the joint synovium is a hallmark of disease, with neutrophils being the most abundant cells found in the inflamed tissue [2,3]. Activated neutrophils promote chronic inflammation as well as matrix and cartilage degradation [3]. Although effective therapies for RA have recently been introduced, unfortunately they are not effective in a significant fraction of the patients [4]. Genome-wide association studies (GWAS) have identified many genetic loci associated with RA; however, most of them are characterized by the presence of single nucleotide polymorphisms (SNPs) in non-coding genetic regions that function in unknown cell types [5]. Therefore, a better understanding of causative and disease contributing factors is still critically needed.

Cell death via apoptosis occurs as a part of homeostasis and during tissue inflammation [6]. Although apoptotic cells have been detected in the synovial joints of rheumatoid arthritis patients [7-9], resistance to apoptosis has also been implied as a contributory factor to chronic disease; therefore, substantial consideration is also given to the induction of apoptosis as a therapeutic avenue in arthritis [10-12]. For evaluation of the potential treatment approaches to increase apoptosis of cells in the arthritic joint, one needs to also consider the specific apoptotic cell clearance pathways.

Apoptotic cells expose 'eat me' signals on their surface that are recognized by specific receptors on phagocytes [13-16]. Binding of apoptotic cells to the phagocyte recognition receptors results in activation of the engulfment machinery, dynamic changes of the actin cytoskeleton, and corpse uptake [13-15]. Many phagocyte proteins have been implicated in the binding of apoptotic cells. They include receptors that bind phosphatidylserine exposed on the apoptotic cell surface directly (such as TIM-4 [17-19] and BAI1 [20]) or indirectly, through bridging molecules (such as MerTK[21]), as well as receptors that recognize cell surface modifications or opsonins bound to the apoptotic cells such as CD36 [22]. The reasons for having many different recognition modes and the specific signaling pathways downstream of these engulfment receptors are

currently unclear and are intensely investigated [23]. One of the better characterized cytoplasmic signaling relays that functions downstream of multiple apoptotic cell engulfment receptors (in both professional and non-professional phagocytes) is the ELMO/DOCK/Rac signaling pathway [24]. In this mode of signaling, the ELMO/DOCK protein complex acts as a guanine nucleotide exchange factor (GEF) to activate the small GTPase Rac, leading to cytoskeletal rearrangements needed for engulfment [25]. Inefficient clearance of apoptotic cells can result in secondary necrosis and exposure of self-antigens to the immune system, and failures in cell clearance have been associated with chronic inflammation and development of autoimmunity [16,26-28].

In this work, we examined how components of a specific engulfment pathway may link to inflammatory arthritis. Surprisingly, we found that the loss of engulfment signaling protein ELMO1 alleviated, rather than enhanced, disease severity in mouse models of arthritis. Through a series of *in vitro* and *in vivo* studies, we define a role for the ELMO1 signaling pathway in the recruitment of neutrophils into inflamed joints. Further, we find that even after onset of arthritis, deletion of ELMO1 can be beneficial in attenuating disease severity. Lastly, we identify a novel ELMO1-dependent signature in neutrophils via proteomic and transcriptomic approaches, and identify a requirement for ELMO1 in signaling downstream of the receptors for arthritis-associated molecules C5a and LTB4. We also uncover a functional consequence of the arthritis-associated *ELMO1* SNP rs11984075 in human neutrophil migration. Collectively, these data identify non-canonical roles for apoptotic cell engulfment components, a novel neutrophil-specific ELMO1-dependent signaling nexus that controls different aspects of arthritis, and link a specific human SNP *ELMO1* rs11984075 to enhanced migration of neutrophils.

RESULTS

Engulfment protein ELMO1 is associated with arthritis

To test whether specific engulfment machinery components are associated with human rheumatoid arthritis, we searched the publicly available databases for single nucleotide polymorphisms (SNPs) associated with human rheumatoid arthritis. We found multiple SNP-Disease associations with human rheumatoid arthritis in *ELMO1*, as well as in *DOCK2* and *RAC1* genes (see *Methods*; ***Fig. 1a*** and *Supplementary Table 1*). In a recent meta-analysis looking for common SNPs or gene linkages to both rheumatoid arthritis (RA) and celiac disease (CD), a SNP in human ELMO1 (rs11984075) was found to be highly correlative with a pre-disposition to developing RA [29]. Further, in an omics-based approach assessing the methylation status of arthritis associated genes, the genetic locus containing *Elmo1* was hypo-methylated in fibroblast-like synoviocytes (FLS) that line the synovium of the joints [30 31]. ELMO1 functions at the interface between the phagocytic receptors and their downstream cytoplasmic signaling activity leading to corpse internalization. Our initial hypothesis was that, as ELMO1 is linked to clearance of apoptotic cells, a process that is generally anti-inflammatory, disruption of ELMO1 might lead to greater inflammation in the joints.

To test whether expression of specific engulfment machinery components might change during joint inflammation in mice, we initially analyzed the K/BxN mouse model of spontaneous arthritis [32] (*Supplementary Fig. 1a*). By approximately one month of age, the K/BxN mice develop spontaneous and progressive joint disease resembling rheumatoid arthritis, including autoantibody production, chronic joint inflammation, and bone erosion [32]. We analyzed expression of the engulfment receptors *Bai1, Bai2, Bai3*, *Tim4*, *Mertk* and *Cd36* as well as the cytoplasmic *Elmo*/*Dock*/*Rac* signaling components in the paw extracts of 9-week old K/BxN mice by qPCR. Interestingly, in the K/BxN mice, we only found increased transcript levels for *Elmo1*, *Rac1* and *Rac2*, while the expression of engulfment receptors either remained unchanged, or was slightly decreased (***Fig. 1b*** and *Supplementary Fig. 1b*). We noted increased expression of ELMO1 protein in immunoblot analysis of paw extracts from mice with spontaneous arthritis (consistent with their increased mRNA levels for *Elmo1*) (***Fig. 1c-d***). Based on this observation and the linkage of ELMO1 SNPs to human rheumatoid arthritis, we addressed the role of ELMO1 further.

Elmo1$^{-/-}$ mice show reduced arthritis severity in two different arthritis models

Transferring serum from arthritic K/BxN mice to healthy mice initiates joint disease that mimics features of human arthritis in many strains of mice [33]. The K/BxN serum transfer arthritis is thought to model the effector phase of human arthritis ('inflammatory flare-ups'), due to the transient nature and strict dependence on the innate immune system. Disease induction is rapid, synchronous, and nearly 100% penetrant, with swelling of the paws apparent 1-2 days post K/BxN serum injection [33]. *Elmo1*$^{-/-}$ mice are generally healthy when housed under specific pathogen free conditions [34,35], and we tested arthritis development in these mice using the serum transfer model via two injections (on day 0 and day 2) of the K/BxN serum (***Fig. 1e***). Extracts from diseased paws of control mice (but not the *Elmo1*$^{-/-}$ mice) showed increased ELMO1 protein levels in the joints during arthritis-associated inflammation (***Fig. 1f***, lanes 1-4). We next assessed arthritis in *Elmo1*$^{-/-}$ mice and their control littermates using paw swelling and other disease parameters to assign clinical scores (see *Methods*) (note: all of the scoring was performed by an investigator blinded to the mouse genotypes until the end of the experimental duration). While arthritis was readily observed and comparable in wild type and heterozygous *Elmo1*$^{+/-}$ mice, surprisingly, homozygous *Elmo1*$^{-/-}$ mice showed significantly milder disease (***Fig. 1g***). At disease maximum (day 10 after the first K/BxN serum injection), *Elmo1*$^{-/-}$ mice had very mild or no paw swelling compared to the littermate controls (***Fig. 1h***). Histology of ankle sections (at day 10) revealed severe inflammatory cell infiltration in control littermates that was significantly decreased in *Elmo1*$^{-/-}$ mice (***Fig. 1i***). These data suggest that the loss of ELMO1 attenuates disease severity in the K/BxN serum transfer model of arthritis. The reduction in disease severity in *Elmo1*$^{-/-}$ mice was also observed with a single injection of K/BxN serum and was not sex-dependent (data not shown). Since two injections of K/BxN serum induced stronger disease (attenuated by ELMO1 deficiency), we have used the two-injection regimen in the rest of this work.

We also tested whether ELMO1 plays a role in another commonly used arthritis model - collagen-induced arthritis (CIA), that mimics many features of human rheumatoid arthritis [36,37], and includes involvement of both the innate and adaptive arms of immunity. We back-crossed *Elmo1*$^{-/-}$ mice to the DBA/1J strain, in which collagen-induced arthritis is most consistently seen [38,39], and immunized them with collagen (see *Methods*) (***Fig. 1j***). Again, we noted increased

ELMO1 protein levels in the paws of control mice with CIA (but not in the *Elmo1*$^{-/-}$ mice) (***Fig. 1k***). While *Elmo1*$^{+/+}$DBA mice developed signs of arthritis around day 21, with most mice becoming sick by about 40 days following immunization, remarkably, about a quarter of *Elmo1*$^{-/-}$ DBA mice displayed no signs of arthritis throughout the duration of the experiment (***Fig. 1l*** and *Supplementary Fig. 1c, 1e*). Moreover, among the mice that did develop arthritis symptoms, *Elmo1*$^{-/-}$DBA mice had delayed onset and significantly reduced disease severity compared to *Elmo1*$^{+/+}$DBA and *Elmo1*$^{+/-}$DBA mice (***Fig. 1m*** and *Supplementary Fig. 1d, 1f*). This difference persisted through the chronic stages of disease in both sexes (*Supplementary Fig. 1c-f*). These data collectively suggest that ELMO1 positively regulates disease severity in arthritis.

ELMO1 function in neutrophils contributes to disease severity in arthritis

When we assessed the presence of uncleared apoptotic cells in the arthritic joints, many cleaved caspase-3 positive cells could be seen in the inflammatory infiltrates of the control littermates (***Fig. 2a***, left panel and inset). Surprisingly, very few such cells were observed in the *Elmo1*-null mice (***Fig. 2a***). Since the fewer apoptotic cells could potentially be linked to the overall reduced inflammation within the joints of *Elmo1*-null mice, we focused on the areas of inflammation; even then, there were significantly fewer apoptotic cells (***Fig. 2a***, right panel). This reduction in apoptotic cells was not due to compensatory upregulation of the homologues *Elmo2* and *Elmo3* in the *Elmo1*$^{-/-}$ mice (*Supplementary Fig. 1g*). During apoptotic cell clearance, ELMO1 binds to the cytoplasmic tail of the phosphatidylserine receptor BAI1, and via subsequent downstream signaling, promotes corpse engulfment (*Supplementary Fig. 1h*) [20]. Interestingly, *Bai1*$^{-/-}$ mice developed comparable disease to their wild type littermates in K/BxN serum induced arthritis model (*Supplementary Fig. 1i*). These data suggest that the attenuation of arthritis seen in *Elmo1*$^{-/-}$ mice is likely not linked to cell clearance *per se*.

We then took a genetic approach to address the cell type(s) in which ELMO1 function was promoting arthritis. Disease development in the K/BxN serum transfer arthritis requires cells of the innate immune system [33]. Since ELMO1 protein expression was detected in both macrophages and neutrophils (***Fig. 2b***), we generated mice with conditional deletion of ELMO1 broadly in the myeloid lineage by crossing *Elmo1*$^{fl/fl}$ mice [34] with LysM-Cre mice, which express Cre recombinase under the *LysM* promoter [40]. When injected with K/BxN serum,

LysM-Cre/*Elmo1*$^{fl/fl}$ mice showed significantly attenuated disease (***Fig. 2c***). Histological examination at disease maximum also revealed reduced inflammation in the ankle joints of LysM-Cre/*Elmo1*$^{fl/fl}$ mice (***Fig. 2d***), and correlated with the loss of ELMO1 protein in myeloid lineage cells (*Supplementary Fig. 2a*). Of note, LysM-Cre expression alone (without floxed *Elmo1* alleles) does not alter disease development in the K/BxN serum induced arthritis (*Supplementary Fig. 2b*). These data suggest that ELMO1 expression in myeloid cells regulates arthritis severity.

Analyzing the cellular composition of the inflammatory infiltrate within the paws, fewer CD11b^{+}Ly6G^{+} neutrophils were seen at disease maximum in the global *Elmo1*$^{-/-}$ mice, as well as the LysM-Cre/*Elmo1*$^{fl/f}$ mice (***Fig. 2e***, *Supplementary Fig. 2c-d*). This indicated a possible link between ELMO1 expression and neutrophil infiltration into the inflamed synovial tissue. To test the importance of ELMO1 expression in neutrophils versus macrophage/monocytic lineages, we crossed *Elmo1*$^{fl/fl}$ mice with either MRP8-Cre mice to delete *Elmo1* expression primarily in neutrophils [41], or CX3CR1-Cre mice, which primarily targets monocytes/macrophages [42,43]. Interestingly, CX3CR1-Cre/*Elmo1*$^{fl/fl}$ mice developed disease comparable to wild type littermates after K/BxN serum injection (***Fig. 2f*** and *Supplementary Fig. 2e-f*), despite decreased ELMO1 protein levels in the macrophage lineage (***Fig. 2g***). On the other hand, deletion of *Elmo1* in neutrophils in the MRP8-Cre/*Elmo1*$^{fl/fl}$ mice led to reduced disease (***Fig. 2h*** *and Supplementary Fig. 2g*). Histological examination of ankle joints showed reduced inflammatory cell infiltration in MRP8-Cre/*Elmo1*$^{fl/fl}$ mice (***Fig. 2i***). ELMO1 deficiency in neutrophils from MRP8-Cre/*Elmo1*$^{fl/fl}$ mice was verified by immunoblot analysis of purified Ly6G^{+} cells (*Supplementary Fig. 2h*). Thus, reduced arthritis induction in MRP8-Cre/*Elmo1*$^{fl/fl}$ mice phenocopies the global *Elmo1*-null mice (***Fig. 2h*** and ***1g***). Importantly, Cre expression alone (via *MRP8* promoter in neutrophils) does not reduce disease severity (*Supplementary Fig. 2i* and data not shown). Since ELMO1 expression was previously reported in fibroblast-like synoviocytes (FLS) [30], we considered the possibility that MRP8-Cre/*Elmo1*$^{fl/fl}$ mice might have affected these cells. However, even in control mice, ELMO1 protein was barely detectable in the FLS (compared to the strong expression in neutrophils that is lost in MRP8-Cre/*Elmo1*$^{fl/fl}$ cells) (*Supplementary Fig. 2j*). Thus, the attenuated disease in MRP8-Cre/*Elmo1*$^{fl/fl}$ mice during K/BxN serum induced arthritis appears to be due to the loss of ELMO1 function in neutrophils.

To address whether ELMO1 may function as a broad inhibitor of inflammation, we used several models of inflammation associated with neutrophil infiltration. First, we challenged *Elmo1*$^{+/+}$ and *Elmo1*$^{-/-}$ mice with intranasal administration of LPS and monitored the recruitment of neutrophils to the lung (*Supplementary Fig. 3a*). Eight hours post-LPS administration, significant recruitment of neutrophils was detected in the bronchoalveolar lavage of control mice, and this was not significantly altered in *Elmo1*$^{-/-}$ mice (*Supplementary Fig. 3b*). Second, we tested whether mice with ELMO1 deficiency can combat a severe bacterial infection *in vivo*. We subjected *Elmo1*$^{+/+}$ and *Elmo1*$^{-/-}$ mice to fecal-induced peritonitis (FIP), a model of septic shock[44,45], and assessed neutrophil recruitment into the infected peritoneum, as well as clinical parameters of disease development and survival (*Supplementary Fig. 3c*). Four hours after FIP induction, *Elmo1*$^{-/-}$ mice had comparable neutrophil infiltration as control mice to the site of infection (*Supplementary Fig. 3d*). The transient temperature drop and clinical scores also did not differ between *Elmo1*$^{+/+}$ and *Elmo1*$^{-/-}$ mice (*Supplementary Fig. 3e-f*). Furthermore, the survival of *Elmo1*$^{-/-}$ mice was not different compared to control mice (*Supplementary Fig. 3g*). We also directly tested purified *Elmo1*$^{-/-}$ neutrophils in their ability to kill a bacterial pathogen *Klebsiella pneumoniae*, clearance of which potently depends on neutrophil function [46]. Again, *Elmo1*$^{-/-}$ neutrophils were not impaired in *in vitro* killing of *Klebsiella pneumoniae* (*Supplementary Fig. 3h*). Third, as *Elmo1*$^{-/-}$ mice do not exhibit symptoms associated with autoimmunity when housed under specific pathogen free conditions, we tested these mice in experimental autoimmune encephalomyelitis (EAE), a model of multiple sclerosis [47,48] that involves adaptive immunity and neutrophil function [49]. *Elmo1*$^{-/-}$ mice developed EAE symptoms comparable to control animals, and had similar levels of demyelination (*Supplementary Fig. 3i-j* and data not shown). Collectively, these data suggest that ELMO1 deficiency does not generally impair inflammation, and that there is likely a specificity associated with ELMO1 loss in neutrophils and attenuation of arthritis signs.

ELMO1 regulates neutrophil chemotaxis to inflamed joints

To better understand the differences in arthritis severity due to ELMO1 deletion in neutrophils versus macrophages, and to help decipher how ELMO1 might affect neutrophil function during arthritis, we assessed the ELMO1 protein interactome in neutrophils versus macrophages. We purified Ly6G^{+} neutrophils from the bone marrow and resident peritoneal

macrophages from *Elmo1*$^{+/+}$ and *Elmo1*$^{-/-}$ mice, and performed ELMO1 immunoprecipitation, followed by liquid chromatography mass spectrometry (LC-MS) and proteomics analysis (***Fig. 3a***). Comparison of the proteomics results between *Elmo1*$^{+/+}$ and *Elmo1*$^{-/-}$ mice helped identify ELMO1-specific protein partners (either direct or indirect interaction with ELMO1). Further analysis of ELMO1 protein interactomes in neutrophils versus macrophages (see *Methods*), helped identify the neutrophil-specific ELMO1 protein interaction network composed of 30 proteins (***Fig. 3b*** *and Supplementary Table 2)*. Neutrophil-specific ELMO1 protein interactome was analyzed by STRING (string-db.org) to reveal protein-protein interactions [50]. The known ELMO1 partners DOCK and RAC were added to ***Fig. 3b*** to provide context (highlighted in blue), although DOCK and RAC were found in interactomes of both neutrophils and macrophages. The newly identified neutrophil-specific ELMO1 partners have a range of distinct functions [51-67], and several have known associations with human arthritis (***Fig. 3c***) [68-77].

Interestingly, several of the neutrophil-specific ELMO1 protein partners are linked to the regulation of cell migration (***Fig. 3b-c***), Initial neutrophil recruitment into the synovium during arthritis is mediated by leukotriene B4 (LTB4) and further sustained by CXCR2 agonists such as CXCL1 [78,79]. As ELMO1 has also been linked to gradient dependent migration [80-83], we examined migration of purified neutrophils from WT and ELMO1-deficient mice in a Transwell migration assay. *Elmo1*$^{-/-}$ neutrophils showed significantly reduced migration toward LTB4 and CXCL1 (***Fig. 3d***). This reduced migration was not a purification related phenomenon, as reduced migration of *Elmo1*-deficient neutrophils toward LTB4 and CXCL1 was also seen when total bone marrow cells were used (*Supplementary Fig. 4a*). To visualize the linkage between ELMO1 expression and neutrophil migration *in vivo*, we used two-photon microscopy to analyze neutrophil swarming towards the site of laser-induced injury in the mouse ear (which is also LTB4-dependent [84]). Compared to wild type neutrophils showing increased and directed migration toward the site of injury, *Elmo1*$^{-/-}$ neutrophils did not effectively move to the injury site and did not increase the speed of movement (***Fig. 3e-f*** and *Movie S1*).

Since neutrophil migration into the joint synovium is a hallmark of acute inflammatory episodes in human rheumatoid arthritis, and is also a requirement for disease development in the K/BxN serum induced arthritis model [3,85,86], we asked whether ELMO1 might affect neutrophil migration to the joints. *Elmo1*$^{+/-}$ and *Elmo1*$^{-/-}$ mice were injected with K/BxN serum, and

neutrophil infiltration into the joints was imaged via IVIS scanning after 24hr by the luminescent signal that arises from the myeloperoxidase-mediated conversion of injected luminol [87,88]. Compared to control animals, *Elmo1*$^{-/-}$ mice had much reduced luminescence in the joints after K/BxN serum injection (***Fig. 4a***). Reduced migration of *Elmo1*-deficient neutrophils was not due to altered expression of the receptors for the chemokines LTB4 or CXCL1, as *Elmo1*$^{-/-}$ neutrophils expressed comparable levels of the LTB4 receptor (*Blt1*) transcript to those observed in *Elmo1*$^{+/+}$ cells (*Supplementary Fig. 4b*), and the protein levels of the CXCL1 receptor CXCR2 were unchanged on the surface of neutrophils in both blood and bone marrow (*Supplementary Fig. 4c*).

ELMO1 acts as a relay between chemokine receptors and neutrophil activation/migration

The above data demonstrated that ELMO1 regulates neutrophil migration *in vitro* and *in vivo,* and in response to chemokines linked to arthritis. As neutrophil migration to other inflammatory stimuli (such as LPS stimulation, or bacterial infection) was not affected by loss of ELMO1, one possible mechanistic explanation was that ELMO1 might function downstream of receptor(s) for arthritis-linked chemokines. Therefore, we mined our proteomics data for potential ELMO1 associated membrane proteins linked to arthritis (***Fig. 3b-c***). We identified two novel ELMO1-binding membrane proteins, both of which have been previously linked to human neutrophil activation/migration to inflamed joints - C5aR1/CD88, receptor for the complement component C5a (also called anaphylatoxin), and the integrin CD11b/Itgam (***Fig. 3b***, highlighted in yellow)[72,89-92].

C5a/C5aR1 is referred to as a "master switch" in neutrophil recruitment that drives establishment of clinical signs of disease in arthritis [86,93,94]. Of note, C5a/C5aR1 signaling does not appear to regulate disease phenotypes in EAE or LPS challenge models [95-97], which we also found are not influenced by ELMO1 deficiency (*Supplementary Fig. 3*). In arthritis, C5aR1 ligation is uniquely required for initial neutrophil adhesion to the endothelium and firm arrest, and is mediated via upregulation of integrins on the neutrophil surface, such as CD11b (our second ELMO1 binding partner of interest) [98]. CD11b is also a classic neutrophil activation marker that is upregulated by different stimuli to regulate migration, including during LTB4-dependent neutrophil swarming [84]. Therefore, we next asked whether CD11b cell surface

exposure induced by neutrophil activation with C5a or LTB4 would be altered due to ELMO1 deficiency (***Fig. 4b***). CD11b levels on wild type neutrophils were strongly increased by C5a or LTB4 stimulation (***Fig. 4c-d***), and this was significantly stunted in *Elmo1*$^{-/-}$ neutrophils (***Fig. 4d***), suggesting that ELMO1 may function in a signaling relay (i.e. inside-out signaling) between neutrophil activation and CD11b integrin-mediated cell adhesion. As control, we did not observe differences in LTB4 or C5a receptor expression, or ligand-dependent C5aR1 internalization in *Elmo1*$^{-/-}$ neutrophils (***Fig. 4e***). We then asked whether CD11b is required for neutrophil migration in response to LTB4. Blocking CD11b function with a neutralizing antibody reduced neutrophil migration to the levels observed in *Elmo1*$^{-/-}$ cells (***Fig. 4f***), suggesting that ELMO1 regulation of neutrophil migration to LTB4 is in part dependent on CD11b. ELMO1-deficient neutrophils were not inherently deficient in CD11b upregulation, as bypassing receptor-mediated activation by a strong intracellular stimulus such as PMA resulted in comparable CD11b increase between *Elmo1*$^{+/+}$ and *Elmo1*$^{-/-}$ neutrophils (***Fig. 4g***, left panel).

We also tested the specificity of ELMO1 for CD11b upregulation/migration in response to arthritis-associated chemokines LTB4 and C5a versus other stimuli. We observed a poor induction of CD11b levels by bacterially derived LPS in neutrophil sufficient or deficient for ELMO1, even upon exposure to a high concentration of LPS (***Fig. 4g***, right panel). We also examined CD11b induction with aggregated IgG (to mimic immune complexes), and found that CD11b was comparably upregulated in WT and *Elmo1*$^{-/-}$ neutrophils (***Fig. 4h***). Furthermore, immune complex mediated neutrophil degranulation and release of chemotactic factors was also not impaired by ELMO1 deficiency, as determined by migration of wild type neutrophils to the chemotactic mediators present in the supernatants from IgG-activated *Elmo1*$^{-/-}$ neutrophils (***Fig. 4i***). It is worth noting that we found no alterations in the surface levels of neutrophil receptors FcγRIII and FcγRIV [88,93,99], or the protein tyrosine kinase Syk that is required for Fcγ receptor signaling [100], in *Elmo1*$^{-/-}$ neutrophils from blood and bone marrow (*Supplementary Fig. 4d-f*). Collectively, these data suggest that ELMO1 is part of the signaling relay that occurs between specific arthritis-associated chemokines (such as C5a and LTB4) and the neutrophil activation marker CD11b linked to neutrophil migration.

Induced deletion of *Elmo1* after disease onset reduces arthritis severity

To test whether deletion of *Elmo1* after induction of arthritis can alleviate disease parameters, we crossed *Elmo1*$^{fl/fl}$ mice with Ubc-Cre^{ERt2} mice, in which the Cre-recombinase is expressed ubiquitously; however, the ERt2-Cre stays functionally inactive due to its fusion with an ER-domain until the administration of tamoxifen, which induces activation of Cre, and this can be done in adult mice at the desired time [101]. After verifying that *Elmo1* deletion in Ubc-Cre^{ERt2}/*Elmo1*$^{fl/fl}$ mice does not occur prior to the administration of tamoxifen (data not shown), we first induced arthritis in Ubc-Cre^{ERt2}/*Elmo1*$^{fl/fl}$ and littermate controls by injection of K/BxN serum on days 0 and 2 (***Fig. 4j***). Starting on day 3, we administered tamoxifen (see *Methods*) to induce *Elmo1* deletion, and monitored disease parameters. Tamoxifen administration in arthritic Ubc-Cre^{ERt2}/*Elmo1*$^{fl/fl}$ mice resulted in the rapid arrest of further disease development and enhanced recovery in both sexes (***Fig. 4k*** and *Supplementary Fig. 5a*), compared to tamoxifen-treated littermate control mice. Since only a partial loss of ELMO1 protein expression was observed in peritoneal and bone marrow cells from Ubc-Cre^{ERt2}/*Elmo1*$^{fl/fl}$ mice (***Fig. 4l***), this suggests that even partial reduction in ELMO1 during acute phases of arthritis could be of benefit. Importantly, Ubc-Cre^{ERt2}/*Elmo1*$^{fl/fl}$ mice did not have reduced disease if tamoxifen was not administered and deletion of *Elmo1* was not induced (*Supplementary Fig. 5b*).

To further test the hypothesis that ELMO1 contributes to the early recruitment of neutrophils to the joint, we deleted *Elmo1* during the peak of K/BxN serum induced arthritis, after the neutrophil mobilization has already occurred (*Supplementary Fig. 5c*). When induced by this "late" regimen, loss of ELMO1 did not significantly improve signs of disease (*Supplementary Fig. 5d*), suggesting that ELMO1 function contributes to the early stages of disease development in this model of arthritis.

***Elmo1* regulates cell type-specific transcriptional programs**

Since Rac1, which functions downstream of ELMO1, has been shown to regulate gene transcription, we next asked if ELMO1 regulates transcriptional networks by RNA-seq analysis. In addition to comparing the gene expression of cells with or without ELMO1, we compared the transcriptomes of neutrophils and macrophages to identify neutrophil-specific ELMO1-dependent transcriptional signatures (***Fig. 5a***). In both cell types, modulators of actin

cytoskeleton dynamics and cell adhesion/migration were regulated by *Elmo1* (*Supplementary Table 3*). However, we noted a clear difference in the prominent classes of functionally related transcripts between the two cell types analyzed. There was an overall paucity of shared genes and transcriptional programs regulated by *Elmo1*, suggesting a previously unappreciated cellular specificity in *Elmo1*-dependent gene networks. *Elmo1*-regulated transcriptomes in neutrophils and macrophages overlapped in only ten genes (including *Elmo1* itself) (***Fig. 5b*** and *Supplementary Table 3*). Remarkably, we find that *Elmo1* deficiency in neutrophils associates with decreased expression of arthritis-promoting factors and increased expression of protective modulators (***Fig. 5c-d***), with many of the *Elmo1*-dependent neutrophil-specific genes having been previously linked to arthritis disease progression [102-114] (***Fig. 5b-d***). Moreover, neutrophils lacking ELMO1 exhibited an anti-inflammatory signature (***Fig. 5b*** and *Supplementary Table 3*), exemplified by the marked up-regulation of the gene *Tnfaip1*, which encodes A20, a potent inhibitor of NFκB signaling, whose loss in myeloid cells has been shown to lead to the development of spontaneous arthritis in mice [115 116].

ELMO1 SNP rs11984075 alters neutrophil migration

When we took a closer look at the *ELMO1* locus for SNP-disease associations, we found multiple SNPs correlating with diabetic nephropathy, IgG glycosylation, celiac disease, and psoriasis, in addition to rheumatoid arthritis (***Fig. 6a***). Although none of the RA-associated SNPs in *ELMO1* have been reported to cause changes in *mRNA* or protein expression, *Elmo1* expression levels were altered in a mouse model of diabetic nephropathy [117]. ELMO1 protein expression is readily detected in human peripheral blood neutrophils *(Supplementary Fig. 5e)*. To examine whether the presence of rheumatoid arthritis-associated SNPs in *ELMO1* may alter ELMO1 protein levels and neutrophil functions, we screened genomic material from 15 healthy blood donors for the presence of *ELMO1* rs11984075 and *ELMO1* rs10488029 (see *Supplementary Table 1*). Two of the fifteen donors were heterozygous for the *ELMO1* rs11984075 (***Fig. 6b***), whereas none bore *ELMO1* rs10488029 (data not shown). ELMO1 protein expression in neutrophils from the two *ELMO1* rs11984075 donors was elevated ~20% when compared to wild type cells (***Fig. 6c***), suggesting the possibility that this intronic mutation could have additional effects on gene expression [118]. Remarkably, neutrophils from the two *ELMO1* rs11984075 donors displayed *increased* migration toward LTB4 in a Transwell assay

(***Fig. 6d***) and had elevated levels of L-selectin/CD62L, a leukocyte receptor that mediates early stages of adhesion to the vascular endothelium during neutrophil extravasation and contributes to disease development in mouse models of arthritis [119,120] (***Fig. 6e***). This was particularly interesting, as we also found significantly reduced levels of CD62L on the surface of circulating neutrophils in *Elmo1*$^{-/-}$ mice (***Fig. 6f***), suggesting an additional putative avenue for ELMO1 regulation of neutrophil recruitment. Since the bone marrow neutrophils from *Elmo1*$^{-/-}$ mice had comparable levels of CD62L ***(Fig. 6g***), loss of ELMO1 likely regulates this adhesion molecule in fully matured neutrophils.

As a complement to this set of observations suggesting a 'gain of function' with rs11984075, we tested whether the *loss* of ELMO1 in human neutrophils affected their migration to arthritis-associated chemokines. Since *ELMO1* depletion in primary human neutrophils is not feasible (due to their short life span), we utilized the human neutrophil cell line HL-60 [121] to analyze whether loss of ELMO1 in human neutrophils would inhibit chemotaxis. HL-60 cells with shRNA mediated knockdown of *ELMO1* expression (***Fig. 6h***) were differentiated into neutrophils (as per [122]) exhibited reduced migration to LTB4 compared to control shRNA expressing cells (***Fig. 6i***). Collectively, these observations demonstrate that ELMO1 modulates human neutrophil chemotaxis to soluble mediators linked to arthritis, suggests that the *ELMO1* rs11984075 mutation may contribute to enhanced neutrophil recruitment to sites of inflammation, and might explain the potential association of this SNP with rheumatoid arthritis.

DISCUSSION

Identification of ELMO1 as a multi-pronged contributory factor for arthritis

Rheumatoid arthritis affects 1% of the human population. While the recent emergence of biologics targeting specific inflammatory components have clearly revolutionized the control of disease symptoms, they have been effective in only a fraction of patients [4]. Thus, this work identifying the ELMO1-dependent molecular signaling nexus with linkages to human arthritis may provide additional new targets for therapeutic intervention. The combination of tissue specific mouse knockout studies, identification of ELMO1 protein interactome, and transcriptomic analyses revealed that ELMO1 serves an important signaling nexus in neutrophils. Moreover, many of the genes/proteins regulated in an ELMO1-dependent manner are genetically linked to human arthritis (via SNPs, altered expression, or biomarker status), or functionally linked to experimental arthritis in animal models. Specifically, we identify an ELMO1-dependent signature in neutrophils via unbiased approaches, and uncover a novel requirement for ELMO1 in the inside-out signaling downstream of the receptors for arthritis-associated molecules C5a and LTB4, involving regulation of the surface expression of CD11b, another key modifier of neutrophil migration to inflamed tissues.

Since K/BxN serum induced arthritis primarily depends on the innate immune system (mimicking the inflammatory flare-ups associated with arthritis), and the CIA depends on both the innate and adaptive immunity arms [123], ELMO1 appears to contribute to arthritis progression in both acute and chronic phases of the disease. Our discovery of enhanced expression of ELMO1 protein in human neutrophils from humans carrying the SNP *ELMO1* rs11984075 and the higher migration of these neutrophils to the chemokine LTB4, which has been linked to early recruitment of neutrophils to the joints, further imply a key linkage of SNPs in ELMO1 to human arthritis at a functional and genetic level. Consistent with the diminished migration of human neutrophils lacking ELMO1 to LTB4, and the observation in mice that deletion of ELMO1 after arthritis initiation could dampen disease symptoms, suggest that targeting ELMO1 function in human arthritis may be an avenue to explore in future studies. Since our data suggest that ELMO1 deficiency does not impair the neutrophil response to bacterial challenge, such approaches may not suppress the immune system indiscriminately.

Rethinking the engulfment machinery in the initiation and resolution of inflammation

A significant amount of data (from many laboratories, including ours) suggest that the apoptotic cell clearance process is generally anti-inflammatory. Therefore, when we initially noticed SNPs and disease associations of ELMO/DOCK/Rac module with rheumatoid arthritis, we hypothesized that this is because of failed apoptotic cell clearance in the arthritic joints (due to the absence of this signaling module). However, unexpectedly and strikingly, the data accumulated through this work (e.g. the SNP *ELMO1* rs11984075 and the mouse knockout studies identifying ELMO1 function in neutrophil migration) advance a concept that evolutionarily conserved apoptotic cell engulfment machinery components can have both canonical and non-canonical roles in inflammation and in different cell types [124-126]. Since induction of apoptosis in rheumatoid tissues has been proposed as a potential therapeutic approach [10-12], our data suggest that careful examination of apoptotic cell engulfment machinery components required for the removal of apoptotic cells should also be characterized in specific inflammatory contexts.

Defining shared and unique gene signatures in neutrophils and macrophages

In comparing the transcriptomics of neutrophils and macrophages from ELMO1 sufficient and deficient conditions, we had a few surprises. First, there were many genes that were uniquely altered by the absence of ELMO1 in neutrophils and macrophages. Second, there were only ten core genes that were commonly regulated in both cell types. This is in contrast to the 'general assumption' that the same genes/proteins likely perform similar functions in different cell types, especially among cell types that are of the general myeloid lineage. Since many of the unique genes in neutrophils are independently linked to rheumatoid arthritis, these data suggest an interesting notion that targeting common pathways could be a less explored area with potential benefit in specific instances.

AUTHOR CONTRIBUTIONS

Conceptualization, S.A. and K.S.R.; Methodology, S.A. and K.S.R.; Software, J.S.A.P.; Investigation, S.A., J.S.A.P., C.D.L., K.K.P., T-H.K., M.Z., D.A R., T-Y.C., A.M.B., L.S.S., A.H.C., and A.G.; Data Curation, J.S.A.P.; Writing, S.A. and K.S.R.; Resources, A.G., T.P.C., M.K., M.R.E. and K.S.R.; Funding Acquisition, K.S.R.

ACKNOWLEDGEMENTS

The authors thank members of the Ravichandran laboratory for discussions and critical reading of the manuscript, Samantha T. Fleury for assistance with neutrophil purification, and Kyle Koster for assistance with bone marrow preparations. This work is supported by grants to K.S.R. from NIGMS R35GM122542, NIMH (MH096484), NHLBI (P01HL120840), NICHD (HD07498), and the Center for Cell Clearance/University of Virginia School of Medicine, and the Odysseus Award from the FWO, Belgium, and to M.R.E. from NIAID (AI114554). Additional support was provided by the Philip S. Magaram, Esq. Research Award from the Arthritis Foundation to S.A., and K.K.P. is supported by an NHLBI F30 award (F30 HL126385) and previously by the NIH T32 Immunology Training Grant (T32 AI007496).

REFERENCES

1 McInnes, I. B. & Schett, G. The pathogenesis of rheumatoid arthritis. *The New England journal of medicine* **365**, 2205-2219, doi:10.1056/NEJMra1004965 (2011).

2 Weissmann, G. & Korchak, H. Rheumatoid arthritis. The role of neutrophil activation. *Inflammation* **8 Suppl**, S3-14 (1984).

3 Wright, H. L., Moots, R. J. & Edwards, S. W. The multifactorial role of neutrophils in rheumatoid arthritis. *Nature reviews. Rheumatology* **10**, 593-601, doi:10.1038/nrrheum.2014.80 (2014).

4 Moots, R. J. & Naisbett-Groet, B. The efficacy of biologic agents in patients with rheumatoid arthritis and an inadequate response to tumour necrosis factor inhibitors: a systematic review. *Rheumatology (Oxford)* **51**, 2252-2261, doi:10.1093/rheumatology/kes217 (2012).

5 Ding, J., Eyre, S. & Worthington, J. Genetics of RA susceptibility, what comes next? *RMD Open* **1**, e000028, doi:10.1136/rmdopen-2014-000028 (2015).

6 Arandjelovic, S. & Ravichandran, K. S. Phagocytosis of apoptotic cells in homeostasis. *Nature immunology* **16**, 907-917, doi:10.1038/ni.3253 (2015).

7 Sugiyama, M. *et al*. Localisation of apoptosis and expression of apoptosis related proteins in the synovium of patients with rheumatoid arthritis. *Annals of the rheumatic diseases* **55**, 442-449 (1996).

8 Chou, C. T., Yang, J. S. & Lee, M. R. Apoptosis in rheumatoid arthritis--expression of Fas, Fas-L, p53, and Bcl-2 in rheumatoid synovial tissues. *The Journal of pathology* **193**, 110-116, doi:10.1002/1096-9896(2000)9999:9999<::AID-PATH746>3.0.CO;2-K (2001).

9 Highton, J., Hessian, P. A., Kean, A. & Chin, M. Cell death by apoptosis is a feature of the rheumatoid nodule. *Annals of the rheumatic diseases* **62**, 77-80 (2003).

10 Imai, Y., Kouzmenko, A. & Kato, S. Targeting Fas/FasL signaling, a new strategy for maintaining bone health. *Expert opinion on therapeutic targets* **15**, 1143-1145, doi:10.1517/14728222.2011.600690 (2011).

11 Pope, R. M. Apoptosis as a therapeutic tool in rheumatoid arthritis. *Nature reviews. Immunology* **2**, 527-535, doi:10.1038/nri846 (2002).

12 Liu, H. & Pope, R. M. The role of apoptosis in rheumatoid arthritis. *Current opinion in pharmacology* **3**, 317-322 (2003).

13 Elliott, M. R. & Ravichandran, K. S. The Dynamics of Apoptotic Cell Clearance. *Developmental cell* **38**, 147-160, doi:10.1016/j.devcel.2016.06.029 (2016).

14 Erwig, L. P. & Henson, P. M. Clearance of apoptotic cells by phagocytes. *Cell death and differentiation* **15**, 243-250, doi:10.1038/sj.cdd.4402184 (2008).

15 Gregory, C. D. & Pound, J. D. Microenvironmental influences of apoptosis in vivo and in vitro. *Apoptosis : an international journal on programmed cell death* **15**, 1029-1049, doi:10.1007/s10495-010-0485-9 (2010).

16 Rothlin, C. V., Carrera-Silva, E. A., Bosurgi, L. & Ghosh, S. TAM receptor signaling in immune homeostasis. *Annual review of immunology* **33**, 355-391, doi:10.1146/annurev-immunol-032414-112103 (2015).

17 Kobayashi, N. *et al*. TIM-1 and TIM-4 glycoproteins bind phosphatidylserine and mediate uptake of apoptotic cells. *Immunity* **27**, 927-940, doi:10.1016/j.immuni.2007.11.011 (2007).

18 Miyanishi, M. *et al*. Identification of Tim4 as a phosphatidylserine receptor. *Nature* **450**, 435-439, doi:10.1038/nature06307 (2007).

19 Santiago, C. *et al*. Structures of T cell immunoglobulin mucin protein 4 show a metal-Ion-dependent ligand binding site where phosphatidylserine binds. *Immunity* **27**, 941-951, doi:10.1016/j.immuni.2007.11.008 (2007).

20 Park, D. *et al*. BAI1 is an engulfment receptor for apoptotic cells upstream of the ELMO/Dock180/Rac module. *Nature* **450**, 430-434, doi:10.1038/nature06329 (2007).

21 Lemke, G. Biology of the TAM receptors. *Cold Spring Harbor perspectives in biology* **5**, a009076, doi:10.1101/cshperspect.a009076 (2013).

22 Savill, J. Recognition and phagocytosis of cells undergoing apoptosis. *British medical bulletin* **53**, 491-508 (1997).

23 Penberthy, K. K. *et al*. Context-dependent compensation among phosphatidylserine-recognition receptors. *Scientific reports* **7**, 14623, doi:10.1038/s41598-017-15191-1 (2017).

24 Penberthy, K. K. & Ravichandran, K. S. Apoptotic cell recognition receptors and scavenger receptors. *Immunological reviews* **269**, 44-59, doi:10.1111/imr.12376 (2016).

25 Elmore, S. Apoptosis: a review of programmed cell death. *Toxicologic pathology* **35**, 495-516, doi:10.1080/01926230701320337 (2007).

26 Nagata, S., Hanayama, R. & Kawane, K. Autoimmunity and the clearance of dead cells. *Cell* **140**, 619-630, doi:10.1016/j.cell.2010.02.014 (2010).

27 Poon, I. K. *et al*. Unexpected link between an antibiotic, pannexin channels and apoptosis. *Nature* **507**, 329-334, doi:10.1038/nature13147 (2014).

28 Bosurgi, L. *et al*. Macrophage function in tissue repair and remodeling requires IL-4 or IL-13 with apoptotic cells. *Science* **356**, 1072-1076, doi:10.1126/science.aai8132 (2017).

29 Zhernakova, A. *et al*. Meta-analysis of genome-wide association studies in celiac disease and rheumatoid arthritis identifies fourteen non-HLA shared loci. *PLoS Genet* **7**, e1002004, doi:10.1371/journal.pgen.1002004 (2011).

30 Whitaker, J. W. *et al*. Integrative omics analysis of rheumatoid arthritis identifies non-obvious therapeutic targets. *PloS one* **10**, e0124254, doi:10.1371/journal.pone.0124254 (2015).

31 Lefevre, S., Meier, F. M., Neumann, E. & Muller-Ladner, U. Role of synovial fibroblasts in rheumatoid arthritis. *Current pharmaceutical design* **21**, 130-141 (2015).

32 Kouskoff, V. *et al*. Organ-specific disease provoked by systemic autoimmunity. *Cell* **87**, 811-822 (1996).

33 Korganow, A. S. *et al*. From systemic T cell self-reactivity to organ-specific autoimmune disease via immunoglobulins. *Immunity* **10**, 451-461 (1999).

34 Elliott, M. R. *et al*. Unexpected requirement for ELMO1 in clearance of apoptotic germ cells in vivo. *Nature* **467**, 333-337, doi:10.1038/nature09356 (2010).

35 Lu, Z. *et al*. Phagocytic activity of neuronal progenitors regulates adult neurogenesis. *Nature cell biology* **13**, 1076-1083, doi:10.1038/ncb2299 (2011).

36 Wooley, P. H. The usefulness and the limitations of animal models in identifying targets for therapy in arthritis. *Best practice & research. Clinical rheumatology* **18**, 47-58, doi:10.1016/j.berh.2003.09.007 (2004).

37 Cho, Y. G., Cho, M. L., Min, S. Y. & Kim, H. Y. Type II collagen autoimmunity in a mouse model of human rheumatoid arthritis. *Autoimmunity reviews* **7**, 65-70, doi:10.1016/j.autrev.2007.08.001 (2007).

38 Courtenay, J. S., Dallman, M. J., Dayan, A. D., Martin, A. & Mosedale, B. Immunisation against heterologous type II collagen induces arthritis in mice. *Nature* **283**, 666-668 (1980).

39 Brand, D. D., Latham, K. A. & Rosloniec, E. F. Collagen-induced arthritis. *Nature protocols* **2**, 1269-1275, doi:10.1038/nprot.2007.173 (2007).

40 Clausen, B. E., Burkhardt, C., Reith, W., Renkawitz, R. & Forster, I. Conditional gene targeting in macrophages and granulocytes using LysMcre mice. *Transgenic research* **8**, 265-277 (1999).

41 Passegue, E., Wagner, E. F. & Weissman, I. L. JunB deficiency leads to a myeloproliferative disorder arising from hematopoietic stem cells. *Cell* **119**, 431-443, doi:10.1016/j.cell.2004.10.010 (2004).

42 Ley, K., Miller, Y. I. & Hedrick, C. C. Monocyte and macrophage dynamics during atherogenesis. *Arteriosclerosis, thrombosis, and vascular biology* **31**, 1506-1516, doi:10.1161/atvbaha.110.221127 (2011).

43 Yona, S. *et al*. Fate mapping reveals origins and dynamics of monocytes and tissue macrophages under homeostasis. *Immunity* **38**, 79-91, doi:10.1016/j.immuni.2012.12.001 (2013).

44 Lewis, A. J., Seymour, C. W. & Rosengart, M. R. Current Murine Models of Sepsis. *Surg Infect (Larchmt)* **17**, 385-393, doi:10.1089/sur.2016.021 (2016).

45 Shrum, B. *et al*. A robust scoring system to evaluate sepsis severity in an animal model. *BMC Res Notes* **7**, 233, doi:10.1186/1756-0500-7-233 (2014).

46 Xiong, H. *et al*. Distinct Contributions of Neutrophils and CCR2+ Monocytes to Pulmonary Clearance of Different Klebsiella pneumoniae Strains. *Infect Immun* **83**, 3418-3427, doi:10.1128/IAI.00678-15 (2015).

47 Mendel, I., Kerlero de Rosbo, N. & Ben-Nun, A. A myelin oligodendrocyte glycoprotein peptide induces typical chronic experimental autoimmune encephalomyelitis in H-2b

mice: fine specificity and T cell receptor V beta expression of encephalitogenic T cells. *European journal of immunology* **25**, 1951-1959, doi:10.1002/eji.1830250723 (1995).

48 Bettelli, E. *et al*. IL-10 is critical in the regulation of autoimmune encephalomyelitis as demonstrated by studies of IL-10- and IL-4-deficient and transgenic mice. *J Immunol* **161**, 3299-3306 (1998).

49 Pierson, E. R., Wagner, C. A. & Goverman, J. M. The contribution of neutrophils to CNS autoimmunity. *Clin Immunol*, doi:10.1016/j.clim.2016.06.017 (2016).

50 Szklarczyk, D. *et al*. The STRING database in 2017: quality-controlled protein-protein association networks, made broadly accessible. *Nucleic acids research* **45**, D362-D368, doi:10.1093/nar/gkw937 (2017).

51 Alon, R. & Shulman, Z. Chemokine triggered integrin activation and actin remodeling events guiding lymphocyte migration across vascular barriers. *Experimental cell research* **317**, 632-641, doi:10.1016/j.yexcr.2010.12.007 (2011).

52 Bridges, D. & Moorhead, G. B. 14-3-3 proteins: a number of functions for a numbered protein. *Sci STKE* **2005**, re10, doi:10.1126/stke.2962005re10 (2005).

53 Delclaux, C. *et al*. Role of gelatinase B and elastase in human polymorphonuclear neutrophil migration across basement membrane. *American journal of respiratory cell and molecular biology* **14**, 288-295, doi:10.1165/ajrcmb.14.3.8845180 (1996).

54 Diaz-Alvarez, L. & Ortega, E. The Many Roles of Galectin-3, a Multifaceted Molecule, in Innate Immune Responses against Pathogens. *Mediators of inflammation* **2017**, 9247574, doi:10.1155/2017/9247574 (2017).

55 Germena, G., Volmering, S., Sohlbach, C. & Zarbock, A. Mutation in the CD45 inhibitory wedge modulates integrin activation and leukocyte recruitment during inflammation. *J Immunol* **194**, 728-738, doi:10.4049/jimmunol.1401646 (2015).

56 Gittens, B. R., Bodkin, J. V., Nourshargh, S., Perretti, M. & Cooper, D. Galectin-3: A Positive Regulator of Leukocyte Recruitment in the Inflamed Microcirculation. *J Immunol* **198**, 4458-4469, doi:10.4049/jimmunol.1600709 (2017).

57 Glennon-Alty, L., Hackett, A. P., Chapman, E. A. & Wright, H. L. Neutrophils and redox stress in the pathogenesis of autoimmune disease. *Free Radic Biol Med* **125**, 25-35, doi:10.1016/j.freeradbiomed.2018.03.049 (2018).

58 Gough, R. E. & Goult, B. T. The tale of two talins - two isoforms to fine-tune integrin signalling. *FEBS letters* **592**, 2108-2125, doi:10.1002/1873-3468.13081 (2018).

59 Jin, J. *et al*. Proteomic, functional, and domain-based analysis of in vivo 14-3-3 binding proteins involved in cytoskeletal regulation and cellular organization. *Current biology : CB* **14**, 1436-1450, doi:10.1016/j.cub.2004.07.051 (2004).

60 Kletzien, R. F., Harris, P. K. & Foellmi, L. A. Glucose-6-phosphate dehydrogenase: a "housekeeping" enzyme subject to tissue-specific regulation by hormones, nutrients, and oxidant stress. *FASEB journal : official publication of the Federation of American Societies for Experimental Biology* **8**, 174-181 (1994).

61 Oikonomou, K. G., Zachou, K. & Dalekos, G. N. Alpha-actinin: a multidisciplinary protein with important role in B-cell driven autoimmunity. *Autoimmunity reviews* **10**, 389-396, doi:10.1016/j.autrev.2010.12.009 (2011).

62 Sadik, C. D., Miyabe, Y., Sezin, T. & Luster, A. D. The critical role of C5a as an initiator of neutrophil-mediated autoimmune inflammation of the joint and skin. *Semin Immunol* **37**, 21-29, doi:10.1016/j.smim.2018.03.002 (2018).

63 Sano, H. *et al*. Human galectin-3 is a novel chemoattractant for monocytes and macrophages. *J Immunol* **165**, 2156-2164 (2000).

64 Springer, T. A. Traffic signals for lymphocyte recirculation and leukocyte emigration: the multistep paradigm. *Cell* **76**, 301-314 (1994).

65 Thomas, D. C. The phagocyte respiratory burst: Historical perspectives and recent advances. *Immunology letters* **192**, 88-96, doi:10.1016/j.imlet.2017.08.016 (2017).

66 Wyatt, E. *et al*. Regulation and cytoprotective role of hexokinase III. *PloS one* **5**, e13823, doi:10.1371/journal.pone.0013823 (2010).

67 Yang, X. *et al*. Structural basis for protein-protein interactions in the 14-3-3 protein family. *Proceedings of the National Academy of Sciences of the United States of America* **103**, 17237-17242, doi:10.1073/pnas.0605779103 (2006).

68 Balakrishnan, L. *et al*. Differential proteomic analysis of synovial fluid from rheumatoid arthritis and osteoarthritis patients. *Clin Proteomics* **11**, 1, doi:10.1186/1559-0275-11-1 (2014).

69 Cui, J. *et al*. Rheumatoid arthritis risk allele PTPRC is also associated with response to anti-tumor necrosis factor alpha therapy. *Arthritis and rheumatism* **62**, 1849-1861, doi:10.1002/art.27457 (2010).

70 de Rooy, D. P. *et al*. A genetic variant in the region of MMP-9 is associated with serum levels and progression of joint damage in rheumatoid arthritis. *Annals of the rheumatic diseases* **73**, 1163-1169, doi:10.1136/annrheumdis-2013-203375 (2014).

71 Gheita, T. A., Kenawy, S. A., El Sisi, R. W., Gheita, H. A. & Khalil, H. Subclinical reduced G6PD activity in rheumatoid arthritis and Sjogren's Syndrome patients: relation to clinical characteristics, disease activity and metabolic syndrome. *Mod Rheumatol* **24**, 612-617, doi:10.3109/14397595.2013.851639 (2014).

72 Hornum, L. *et al*. C5a and C5aR are elevated in joints of rheumatoid and psoriatic arthritis patients, and C5aR blockade attenuates leukocyte migration to synovial fluid. *PloS one* **12**, e0189017, doi:10.1371/journal.pone.0189017 (2017).

73 Hu, C. Y., Chang, S. K., Wu, C. S., Tsai, W. I. & Hsu, P. N. Galectin-3 gene (LGALS3) +292C allele is a genetic predisposition factor for rheumatoid arthritis in Taiwan. *Clin Rheumatol* **30**, 1227-1233, doi:10.1007/s10067-011-1741-2 (2011).

74 Huang, R. Y., Huang, Q. C. & Burgering, B. M. Novel insight into the role of alpha-actinin-1 in rheumatoid arthritis. *Discov Med* **17**, 75-80 (2014).

75 Maksymowych, W. P. & Marotta, A. 14-3-3eta: a novel biomarker platform for rheumatoid arthritis. *Clin Exp Rheumatol* **32**, S-35-39 (2014).

76 Tsuzaka K, I. Y., Shinozaki N, and Morishita T. Plasma talin is a new diagnostic and monitoring marker for rheumatoid arthritis. *Arthritis and rheumatism* **S134** (2011).

77 Warchol, T., Lianeri, M., Lacki, J. K., Olesinska, M. & Jagodzinski, P. P. ITGAM Arg77His is associated with disease susceptibility, arthritis, and renal symptoms in systemic lupus erythematosus patients from a sample of the Polish population. *DNA Cell Biol* **30**, 33-38, doi:10.1089/dna.2010.1041 (2011).

78 Chou, R. C. *et al*. Lipid-cytokine-chemokine cascade drives neutrophil recruitment in a murine model of inflammatory arthritis. *Immunity* **33**, 266-278, doi:10.1016/j.immuni.2010.07.018 (2010).

79 de Oliveira, S., Rosowski, E. E. & Huttenlocher, A. Neutrophil migration in infection and wound repair: going forward in reverse. *Nature reviews. Immunology* **16**, 378-391, doi:10.1038/nri.2016.49 (2016).

80 Gumienny, T. L. *et al*. CED-12/ELMO, a novel member of the CrkII/Dock180/Rac pathway, is required for phagocytosis and cell migration. *Cell* **107**, 27-41 (2001).

81 Grimsley, C. M. *et al*. Dock180 and ELMO1 proteins cooperate to promote evolutionarily conserved Rac-dependent cell migration. *The Journal of biological chemistry* **279**, 6087-6097, doi:10.1074/jbc.M307087200 (2004).

82 Lu, M. *et al*. PH domain of ELMO functions in trans to regulate Rac activation via Dock180. *Nat Struct Mol Biol* **11**, 756-762, doi:10.1038/nsmb800 (2004).

83 Brugnera, E. *et al*. Unconventional Rac-GEF activity is mediated through the Dock180-ELMO complex. *Nature cell biology* **4**, 574-582, doi:10.1038/ncb824 (2002).

84 Lammermann, T. *et al*. Neutrophil swarms require LTB4 and integrins at sites of cell death in vivo. *Nature* **498**, 371-375, doi:10.1038/nature12175 (2013).

85 Pittman, K. & Kubes, P. Damage-associated molecular patterns control neutrophil recruitment. *Journal of innate immunity* **5**, 315-323, doi:10.1159/000347132 (2013).

86 Wipke, B. T. & Allen, P. M. Essential role of neutrophils in the initiation and progression of a murine model of rheumatoid arthritis. *J Immunol* **167**, 1601-1608 (2001).

87 Gross, S. *et al*. Bioluminescence imaging of myeloperoxidase activity in vivo. *Nature medicine* **15**, 455-461, doi:10.1038/nm.1886 (2009).

88 Mancardi, D. A. *et al*. Cutting Edge: The murine high-affinity IgG receptor FcgammaRIV is sufficient for autoantibody-induced arthritis. *J Immunol* **186**, 1899-1903, doi:10.4049/jimmunol.1003642 (2011).

89 Andersson, C. *et al*. Rapid-onset clinical and mechanistic effects of anti-C5aR treatment in the mouse collagen-induced arthritis model. *Clin Exp Immunol* **177**, 219-233, doi:10.1111/cei.12338 (2014).

90 Banda, N. K. *et al*. Role of C3a receptors, C5a receptors, and complement protein C6 deficiency in collagen antibody-induced arthritis in mice. *J Immunol* **188**, 1469-1478, doi:10.4049/jimmunol.1102310 (2012).

91 Park-Min, K. H. *et al*. Negative regulation of osteoclast precursor differentiation by CD11b and beta2 integrin-B-cell lymphoma 6 signaling. *J Bone Miner Res* **28**, 135-149, doi:10.1002/jbmr.1739 (2013).

92 Yang, G., Chen, X., Yan, Z., Zhu, Q. & Yang, C. CD11b promotes the differentiation of osteoclasts induced by RANKL through the spleen tyrosine kinase signalling pathway. *J Cell Mol Med*, doi:10.1111/jcmm.13254 (2017).

93 Ji, H. *et al*. Arthritis critically dependent on innate immune system players. *Immunity* **16**, 157-168 (2002).

94 Monach, P. A. *et al*. Neutrophils in a mouse model of autoantibody-mediated arthritis: critical producers of Fc receptor gamma, the receptor for C5a, and lymphocyte function-associated antigen 1. *Arthritis and rheumatism* **62**, 753-764, doi:10.1002/art.27238 (2010).

95 Morgan, B. P., Griffiths, M., Khanom, H., Taylor, S. M. & Neal, J. W. Blockade of the C5a receptor fails to protect against experimental autoimmune encephalomyelitis in rats. *Clin Exp Immunol* **138**, 430-438, doi:10.1111/j.1365-2249.2004.02646.x (2004).

96 Ramos, T. N., Wohler, J. E. & Barnum, S. R. Deletion of both the C3a and C5a receptors fails to protect against experimental autoimmune encephalomyelitis. *Neuroscience letters* **467**, 234-236, doi:10.1016/j.neulet.2009.10.045 (2009).

97 Rittirsch, D. *et al*. Functional roles for C5a receptors in sepsis. *Nature medicine* **14**, 551-557, doi:10.1038/nm1753 (2008).

98 Miyabe, Y. *et al*. Complement C5a Receptor is the Key Initiator of Neutrophil Adhesion Igniting Immune Complex-induced Arthritis. *Sci Immunol* **2**, doi:10.1126/sciimmunol.aaj2195 (2017).

99 Corr, M. & Crain, B. The role of FcgammaR signaling in the K/B x N serum transfer model of arthritis. *J Immunol* **169**, 6604-6609 (2002).

100 Kiefer, F. *et al*. The Syk protein tyrosine kinase is essential for Fcgamma receptor signaling in macrophages and neutrophils. *Molecular and cellular biology* **18**, 4209-4220 (1998).

101 Ruzankina, Y. *et al*. Deletion of the developmentally essential gene ATR in adult mice leads to age-related phenotypes and stem cell loss. *Cell Stem Cell* **1**, 113-126, doi:10.1016/j.stem.2007.03.002 (2007).

102 Cottier, K. E., Fogle, E. M., Fox, D. A. & Ahmed, S. Noxa in rheumatic diseases: present understanding and future impact. *Rheumatology (Oxford)* **53**, 1539-1546, doi:10.1093/rheumatology/ket408 (2014).

103 Cui, J. *et al*. Genome-wide association study and gene expression analysis identifies CD84 as a predictor of response to etanercept therapy in rheumatoid arthritis. *PLoS Genet* **9**, e1003394, doi:10.1371/journal.pgen.1003394 (2013).

104 Elsby, L. M. *et al*. Functional evaluation of TNFAIP3 (A20) in rheumatoid arthritis. *Clin Exp Rheumatol* **28**, 708-714 (2010).

105 Howng, S. L. *et al*. Autoimmunity against hNinein, a human centrosomal protein, in patients with rheumatoid arthritis and systemic lupus erythematosus. *Mol Med Rep* **4**, 825-830, doi:10.3892/mmr.2011.505 (2011).

106 Issuree, P. D. *et al*. iRHOM2 is a critical pathogenic mediator of inflammatory arthritis. *The Journal of clinical investigation* **123**, 928-932, doi:10.1172/JCI66168 (2013).

107 Jin, T., Tarkowski, A., Carmeliet, P. & Bokarewa, M. Urokinase, a constitutive component of the inflamed synovial fluid, induces arthritis. *Arthritis research & therapy* **5**, R9-R17 (2003).

108 Lopez, M. *et al*. Tumor necrosis factor and transforming growth factor beta regulate clock genes by controlling the expression of the cold inducible RNA-binding protein (CIRBP). *The Journal of biological chemistry* **289**, 2736-2744, doi:10.1074/jbc.M113.508200 (2014).

109 Marotte, H. *et al*. Blocking of interferon regulatory factor 1 reduces tumor necrosis factor alpha-induced interleukin-18 bioactivity in rheumatoid arthritis synovial fibroblasts by induction of interleukin-18 binding protein a: role of the nuclear interferon regulatory factor 1-NF-kappaB-c-jun complex. *Arthritis and rheumatism* **63**, 3253-3262, doi:10.1002/art.30583 (2011).

110 Ohyama, K. *et al*. Serum immune complex containing thrombospondin-1: a novel biomarker for early rheumatoid arthritis. *Annals of the rheumatic diseases* **71**, 1916-1917, doi:10.1136/annrheumdis-2012-201305 (2012).

111 Okada, Y. *et al*. Genetics of rheumatoid arthritis contributes to biology and drug discovery. *Nature* **506**, 376-381, doi:10.1038/nature12873 (2014).

112 Perlman, H. *et al*. Rheumatoid arthritis synovial macrophages express the Fas-associated death domain-like interleukin-1beta-converting enzyme-inhibitory protein and are refractory to Fas-mediated apoptosis. *Arthritis and rheumatism* **44**, 21-30, doi:10.1002/1529-0131(200101)44:1<21::AID-ANR4>3.0.CO;2-8 (2001).

113 Rico, M. C. *et al*. Amelioration of inflammation, angiogenesis and CTGF expression in an arthritis model by a TSP1-derived peptide treatment. *Journal of cellular physiology* **211**, 504-512, doi:10.1002/jcp.20958 (2007).

114 Yoo, I. S. *et al*. Serum and synovial fluid concentrations of cold-inducible RNA-binding protein in patients with rheumatoid arthritis. *Int J Rheum Dis*, doi:10.1111/1756-185X.12892 (2016).

115 Catrysse, L., Vereecke, L., Beyaert, R. & van Loo, G. A20 in inflammation and autoimmunity. *Trends in immunology* **35**, 22-31, doi:10.1016/j.it.2013.10.005 (2014).

116 Matmati, M. *et al*. A20 (TNFAIP3) deficiency in myeloid cells triggers erosive polyarthritis resembling rheumatoid arthritis. *Nature genetics* **43**, 908-912, doi:10.1038/ng.874 (2011).

117 Hathaway, C. K. *et al*. High Elmo1 expression aggravates and low Elmo1 expression prevents diabetic nephropathy. *Proceedings of the National Academy of Sciences of the United States of America* **113**, 2218-2222, doi:10.1073/pnas.1600511113 (2016).

118 Cooper, D. N. Functional intronic polymorphisms: Buried treasure awaiting discovery within our genes. *Hum Genomics* **4**, 284-288 (2010).

119 Sarraj, B., Ludanyi, K., Glant, T. T., Finnegan, A. & Mikecz, K. Expression of CD44 and L-selectin in the innate immune system is required for severe joint inflammation in the proteoglycan-induced murine model of rheumatoid arthritis. *J Immunol* **177**, 1932-1940 (2006).

120 Szanto, S., Gal, I., Gonda, A., Glant, T. T. & Mikecz, K. Expression of L-selectin, but not CD44, is required for early neutrophil extravasation in antigen-induced arthritis. *J Immunol* **172**, 6723-6734 (2004).

121 Hauert, A. B., Martinelli, S., Marone, C. & Niggli, V. Differentiated HL-60 cells are a valid model system for the analysis of human neutrophil migration and chemotaxis. *Int J Biochem Cell Biol* **34**, 838-854 (2002).

122 Collins, S. J., Ruscetti, F. W., Gallagher, R. E. & Gallo, R. C. Terminal differentiation of human promyelocytic leukemia cells induced by dimethyl sulfoxide and other polar compounds. *Proceedings of the National Academy of Sciences of the United States of America* **75**, 2458-2462 (1978).

123 Asquith, D. L., Miller, A. M., McInnes, I. B. & Liew, F. Y. Animal models of rheumatoid arthritis. *European journal of immunology* **39**, 2040-2044, doi:10.1002/eji.200939578 (2009).

124 Wu, Y. C. & Horvitz, H. R. C. elegans phagocytosis and cell-migration protein CED-5 is similar to human DOCK180. *Nature* **392**, 501-504, doi:10.1038/33163 (1998).

125 Wu, Y. C., Tsai, M. C., Cheng, L. C., Chou, C. J. & Weng, N. Y. C. elegans CED-12 acts in the conserved crkII/DOCK180/Rac pathway to control cell migration and cell corpse engulfment. *Developmental cell* **1**, 491-502 (2001).

126 Zhou, Z., Caron, E., Hartwieg, E., Hall, A. & Horvitz, H. R. The C. elegans PH domain protein CED-12 regulates cytoskeletal reorganization via a Rho/Rac GTPase signaling pathway. *Developmental cell* **1**, 477-489 (2001).

127 Boyum, A. Isolation of mononuclear cells and granulocytes from human blood. Isolation of monuclear cells by one centrifugation, and of granulocytes by combining centrifugation and sedimentation at 1 g. *Scand J Clin Lab Invest Suppl* **97**, 77-89 (1968).

128 Stohl, E. A., Criss, A. K. & Seifert, H. S. The transcriptome response of Neisseria gonorrhoeae to hydrogen peroxide reveals genes with previously uncharacterized roles in oxidative damage protection. *Mol Microbiol* **58**, 520-532, doi:10.1111/j.1365-2958.2005.04839.x (2005).

129 Armaka, M., Gkretsi, V., Kontoyiannis, D. & Kollias, G. A standardized protocol for the isolation and culture of normal and arthritogenic murine synovial fibroblasts. (2009).

130 Li, M. J. *et al*. GWASdb: a database for human genetic variants identified by genome-wide association studies. *Nucleic acids research* **40**, D1047-1054, doi:10.1093/nar/gkr1182 (2012).

131 Pletscher-Frankild, S., Palleja, A., Tsafou, K., Binder, J. X. & Jensen, L. J. DISEASES: text mining and data integration of disease-gene associations. *Methods* **74**, 83-89, doi:10.1016/j.ymeth.2014.11.020 (2015).

132 Davis, A. P. *et al*. The Comparative Toxicogenomics Database's 10th year anniversary: update 2015. *Nucleic acids research* **43**, D914-920, doi:10.1093/nar/gku935 (2015).

133 Davis, A. P. *et al*. Comparative Toxicogenomics Database: a knowledgebase and discovery tool for chemical-gene-disease networks. *Nucleic acids research* **37**, D786-792, doi:10.1093/nar/gkn580 (2009).

134 Eppig, J. T., Blake, J. A., Bult, C. J., Kadin, J. A. & Richardson, J. E. The Mouse Genome Database (MGD): facilitating mouse as a model for human biology and disease. *Nucleic acids research* **43**, D726-736, doi:10.1093/nar/gku967 (2015).

135 Blake, J. A., Richardson, J. E., Bult, C. J., Kadin, J. A. & Eppig, J. T. MGD: the Mouse Genome Database. *Nucleic acids research* **31**, 193-195 (2003).

METHODS

Mice

C57BL/6J, DBA/1J, NOD, MRP8-Cre, CX3CR1-Cre, LysM-Cre, and Ubc-Cre^{ERt2} mice were obtained from Jackson Laboratories. *Elmo1*$^{fl/fl}$ and *Elmo1*$^{-/-}$ mice have been described previously [34]. To generate mice with deletion of *Elmo1* in myeloid cells, neutrophils or macrophages, *Elmo1*$^{fl/fl}$ mice were crossed to LysM-Cre, MRP8-Cre or CX3CR1-Cre mice, respectively. To generate mice with inducible deletion of *Elmo1*, *Elmo1*$^{fl/fl}$ mice were crossed to Ubc-Cre^{ERt2}. In these mice, *Elmo1* deletion was induced by three daily intraperitoneal injections of 40 mg/kg tamoxifen dissolved in corn oil. To generate *Elmo1*$^{-/-}$DBA mice, *Elmo1*$^{-/-}$ mice were backcrossed onto the DBA/1J background for at least 5 generations. KRN TCR transgenic mice [32] were a gift from Dr. Diane Mathis at the Harvard Medical School, and were bred to NOD mice to obtain the K/BxN mice [33], which develop progressive spontaneous arthritis. K/BxN serum was collected from 9-week old K/BxN mice by cardiac puncture. Age- and sex-matched littermate control animals were used for all experiments, and both males and females were assessed. In LysM-Cre/*Elmo1*$^{fl/fl}$ mice, reduced disease severity was observed in female, but not in male mice (data not shown). All animal procedures were approved by and performed according to guidelines of the Institutional Animal Care and Use Committee (IACUC) at the University of Virginia.

K/BxN serum transfer induced arthritis

Mice were injected with 150 μl of serum from K/BxN mice on day 0 (one dose K/BxN) or on days 0 and 2 (two dose K/BxN). In experiments with inducible deletion of *Elmo1*, tamoxifen was administered on days 3, 4 and 5. Paw swelling was measured at indicated time points using a caliper (Fisher). Clinical scores were assigned for each paw as follows: 0 – no paw swelling or redness observed, 1 – redness of the paw or a single digit swollen, normal V shape of the hind foot (the foot at the base of the toes is wider than the heel and ankle) 2 – two or more digits swollen or visible swelling of the paw, U shape of the hind foot (the ankle and the midfoot are equal in thickness), 3 – reversal of the V shape of the hind foot into an hourglass shape (the foot is wider at the heel than at the base of the toes). A combined clinical score of all paws is presented. Scores were assigned by an investigator blinded to the mouse genotypes. Pictures were taken with the Nikon Lumix camera.

Collagen induced arthritis (CIA)

Elmo1$^{-/-}$ mice in the DBA background were immunized at the base of the tail by intradermal injection of a 1:1 solution of 10 mM acetic acid containing 100 μg of bovine collagen-II and Complete Freund's Adjuvant (Sigma) containing 100 μg of heat killed Mycobacterium tuberculosis H37Ra (BD). Mice received a booster immunization on day 21. Paw swelling was measured at indicated time points using a caliper. Clinical scores were assigned for each paw as follows: 0 – no paw swelling or redness observed, 1 – redness of the paw or a single digit swollen, 2 – two or more digits swollen or visible swelling of the paw, 3 – visible swelling of the ankle, 4 – ankylosis of the joint. A combined clinical score of all paws is presented. Scores were assigned by an investigator blinded to the mouse genotypes.

Experimental autoimmune encephalomyelitis (EAE)

EAE was induced in female mice (8 to 12 weeks) by subcutaneous injection of MOG_{35-55} peptide (100 μg, CSBio) emulsified in complete Freund's adjuvant. Pertussis toxin (250 ng, List Biologicals) was administered i.p. on the day of and 1d after MOG immunization. For clinical evaluation, mice were scored daily according to the following criteria: 0 - no clinical disease, 1 - limp tail, 2 - hind limb weakness, 3 - hind limb paralysis, 4 - hind limb paralysis and partial front limb paralysis, 5 - moribund. Scores were assigned by an investigator blinded to the mouse genotypes.

Histology

For K/BxN serum transfer induced arthritis, mice were euthanized at the indicated time points and the paws were fixed in 10% formalin (Fisher). Decalcification, sectioning, paraffin embedding and hematoxylin and eosin (H&E) staining was performed by HistoTox Labs (Boulder, CO). Histology scoring was performed by an investigator blinded to the mouse genotypes. For inflammation scoring, the following criteria were used - 0, none; 1, mild; 2, moderate; 3, severe. For bone erosion scoring, the following criteria were used: 0, no bone erosions observed; 1, mild cortical bone erosion; 2, severe cortical bone erosion without the loss of bone integrity; 3, severe cortical bone erosion with the loss of cortical bone integrity and trabecular bone erosion. Cleaved caspase-3 staining was performed at the University of Virginia Biorepository and Tissue Research Facility. For RNA and protein isolation, the paws were snap frozen in liquid nitrogen at indicated time points and subjected to mechanical disruption using a tissue pulverizer (Spectrum Laboratories, Inc.). For EAE experiments, spinal cords were isolated

on day 26 after immunization, paraffin embedded and 4 μm sections were cut, stained with Luxol Fast Blue and counterstained with hematoxylin following standard protocols. Extent of demyelination (loss of blue staining) in the white matter of the spinal cord was measured at 4 different levels of the spinal cord.

Flow cytometry of arthritic joints

Mice were injected with the K/BxN serum on day 0 and day 2, as described above. On day 10, mice were euthanized and the skin removed from the hind paws. Ankle tendons were cut and the foot was detached from the tibia and placed in DMEM containing 20 units/ml of collagenase IV (Roche). The soft tissue was cut with a scalpel and the joints opened by gentle pulling of the foot bones. The paws were incubated for 2 hours at 37°C with periodic trituration. Liberated cells were collected, strained though a 70 μm filter (Fisher), washed with DMEM, counted and subjected to flow cytometry on Canto I flow cytometer using 7-aminoactinomycin D (7-AAD) to identify live cells, and anti-CD45 (eBioscience), anti-CD11b (eBioscience) and anti-Ly6G (clone 1A8, BD Pharmingen) antibodies.

Neutrophil isolation, stimulation and *in vitro* migration

Femurs were removed from 6-8 week old mice, flushed with sterile serum-free α-MEM and single cell suspensions were prepared using the 70 μm cell strainer. Cells were incubated with anti-Ly6G antibody (clone 1A8, BD Pharmingen) and purified using the anti-PE MACS kit (Myltenyi), following manufacturer's instructions. Purified neutrophils ($Ly6G^+$) were seeded in 96-well tissue culture U-bottom plates (10^6 cells per well) and stimulated with 100 ng/ml mouse C5a (R and D Systems), 1-10 nM LTB4, 50 ng/ml PMA (Calbiochem) or 0.5-10 μg/ml LPS (*Escherichia coli* 0111:B4, Sigma). Alternatively, high-binding 96-well plates (Greiner Bio-One) were coated with 50 μg/ml of mouse IgG (Southern Biotech) in PBS for 16 hours at 4°C, washed with PBS and purified neutrophils were seeded as above to induce FcγR-mediated neutrophil stimulation. Cells were stimulated for 1 hour at 37°C, and the cells were then washed and stained with antibodies specific for CD11b or CD88/C5aR1 (eBioscience) and subjected to flow cytometry analysis on the Canto I (BD Bioscience) or the Attune Nxt (Thermo Fisher) flow cytometer. In some experiments, supernatants from cells stimulated with IgG were collected by centrifugation and removal of cell pellets and used for migration, as described below. For

migration experiments, total bone marrow (2 x 10^6 cells per well) or purified $Ly6G^+$ bone marrow cells (0.2-0.5 x 10^6 cells per well) were seeded in top chambers of 3 μm polycarbonate Transwell plates (Corning) in 100 μl of HBSS (with calcium and magnesium, no phenol red, Gibco) containing 1% bovine serum albumin (Roche). Bottom chambers contained 600 μl of media without (control) or with the indicated concentrations of leukotriene B4 (LTB4, Tocris Bioscience) or CXCL1 (BioLegend), or undiluted supernatants from IgG-stimulated neutrophils. After 3 hours at 37°C, the cells in the bottom wells were collected and subjected to flow cytometry analysis with counting beads (Spherotech, Inc.). The data is presented as percent of input cells. Alternatively, bone marrow neutrophils were isolated using the EasySep Mouse Neutrophil Enrichment Kit according to manufacturer's instructions (StemCell Technologies, Vancouver, BC).

Intravital imaging of neutrophil motility

To visualize migration of neutrophils, intravital imaging was performed using FV1000-AOM multiphoton system (Olympus) equipped with a 25x NA1.05 water immersion objective. For two-photon excitation, a Mai-Tai HP Ti:Sa Deep See laser system (Spectra-Physics) was tuned to 900nm for imaging. Neutrophils labeled with CellTracker™ Green CMFDA (Thermo Fisher Scientific Inc.) were intradermally injected into ear skin 2h before *in vivo* imaging. Mice were anesthetized by intraperitoneal injection of pentobarbital (Nembutal Sodium solution, Oak Pharmaceuticals, Inc., IL) and anesthetic condition was maintained using isoflurane. Hair of the mouse ear was removed using a commercial hair remover (Nair, Princeton, NJ). The anesthetized mice were laid in a ventral recumbent position on a custom-designed stage to expose the dorsal side of the ear pinna for imaging. Micropore™ (3M health care, MN) tapes were placed to immobilize the ear skin. Body temperature of the mice was controlled with heat pad and the ear immersed in a drop of glycerol/saline (40:60 v/v) and covered with a coverslip. Laser injury was induced by focusing the multiphoton laser tuned to 800 nm at a region within the ear dermis for 5 seconds. To track and analyze the movements of the neutrophils, Volocity software (Improvision/Perkin-Elmer, Waltham, MA) and ImageJ (National Institutes of Health, Bethesda, MD) were used.

LPS challenge and bacterial killing

Elmo1$^{+/+}$, *Elmo1*$^{-/-}$, *Elmo1*$^{fl/fl}$ and MRP8-Cre/*Elmo1*$^{fl/fl}$ mice were anesthetized with isoflurane and 20 μg of LPS was administered intranasally in a 50 μl volume. Eight hours later, mice were euthanized by anesthetic overdose. Post-euthanasia, an incision was made in the trachea and the bronchoalveolar spaces were lavaged with 750 - 1,000 μl of PBS. The bronchoalveolar lavage (BAL) fluid was subjected to flow cytometry using 7-AAD (BD Bioscience), anti-Ly6G-APC (eBioscience clone 1A8), anti-Ly6C-FITC (BD Biosciences clone AL-21), and anti-CD11b-PE-Cy7 (eBioscience clone M1/70). Data was analyzed on the Canto I (BD) or the Attune Nxt (Thermo Fisher) flow cytometer. Counting beads (Spherotech ACBP-50-10) were used to calculate the absolute number of neutrophils in the BAL fluid. For neutrophil-mediated bacterial killing assays, neutrophils from *Elmo1*$^{+/+}$ and *Elmo1*$^{-/-}$ mice were purified from the bone marrow using anti-Ly6G antibodies, as described above. *Klebsiella pneumoniae* strain 43816 (ATCC) was opsonized with heat inactivated, sterile FBS for 30 min at 37°C. Bacteria were washed twice and 200,000 bacteria were added to 100,000 purified neutrophils in a 96-well tissue culture plate for 1 hour at 37°C. In some wells, extracellular bacteria were killed by 1 μg/ml of gentamicin for 10 min at 37°C. Number of surviving bacteria was determined by hypotonic lysis of neutrophils in cold water and serial dilution and culture on blood agar plates.

Fecal-induced peritonitis (FIP)

Fecal material was isolated from the caecum of donor wild type mice, resuspended in saline and passed through a 70μM strainer to remove large particles. Eight-week old male *Elmo1*$^{+/+}$ and *Elmo1*$^{-/-}$ mice were injected intraperitoneally with an LD50 dosage of 1.5mg fecal content/g mouse weight [44,45]. Core body temperature was measured using a MicroTherma 2T handheld thermometer (Braintree Scientific, TW2-107) and mice were scored for clinical signs according to a published murine sepsis severity scale [45]. Some mice were euthanized 4 hours after FIP induction and peritoneal cells were flushed out with PBS containing 5% FBS. Cells were stained with Fixable Yellow (to identify viable cells, Thermo Fisher) and anti-Ly6G (eBioscience clone 1A8) and subjected to flow cytometry on the Attune Nxt flow cytometer (Thermo Fisher).

Human peripheral blood neutrophils

Human neutrophils were kindly provided by Drs. Alison Criss and Asya Smirnov (University of Virginia). Neutrophils were collected from venous blood of de-identified healthy human donors

using dextran sedimentation followed by Ficoll gradient sedimentation and hypotonic lysis as described [127,128]. Buffy coats were also collected and consist of the non-granulocytic cells collected from the Ficoll gradient. Genomic DNA from purified neutrophils was prepared using the MagMax DNA kit (Applied Biosystems) and the status of the *ELMO1* rs11984075 SNP was determined using the TaqMan SNP genotyping assay (Applied Biosystems), following manufacturer's instructions. For Transwell migration assays, 5 x 10^5 cells were seeded in top chambers of 3 μm polycarbonate Transwell plates in 100 μl of HBSS containing 1% bovine serum albumin, as described for mouse neutrophils. Bottom chambers contained 600 μl of 15 nM leukotriene B4. After 2 hours at 37°C, the cells in the bottom wells were collected and subjected to flow cytometry analysis with counting beads (Spherotech, Inc.), TO-PRO-3 iodide (to identify viable cells, Life Technologies), anti-CD16 (eBioscience) and anti-CD11b (BD Pharmingen) on Canto I flow cytometer (BD Bioscience). The data is presented as percent of input cells.

Analysis of human HL-60 cells

HL-60 cell line (ATCC) was grown in IMDM containing 20% FBS (Gemini Bio-Products) and 1% penicillin/streptomycin/glutamine (Gemini Bio-Products). For differentiation into neutrophil-like cells, HL-60 cells were treated with 1.25% DMSO (Sigma) for 4 days and then cultured without DMSO for 16h. For generating *Elmo1* knockdown cells, HL-60 cells were transfected with 10 μg of human *Elmo1* targeting or control shRNA pGFP-V-RS expression vectors (OriGene Technologies, Inc.) using electroporation using a 250 V, 25 ms pulse. After 24h, stably transfected cells were selected with 0.2 μg/ml puromycin (Gibco) and single cell cloning was performed by serial dilution. A total of three control and four *Elmo1* shRNA clones were analyzed. Differentiated cells (1 x 10^5 cells per well) were seeded in top chambers of 3 μm polycarbonate Transwell plates in 100 μl of HBSS containing 1% bovine serum albumin, as described for neutrophils. Bottom chambers contained 600 μl of 100 nM leukotriene B4. After 1 hour at 37°C, the cells in the bottom wells were collected and subjected to flow cytometry analysis, as described above. The data is presented as percent of input cells.

Macrophage cultures

For resident peritoneal macrophage preparation, peritoneal cells were flushed out with PBS containing 5% FBS. Collected cells were spun down, re-suspended in XVIVO-10 (Lonza)

containing 1% penicillin/streptomycin/glutamine and cultured on tissue culture dishes at 37°C and 5% carbon dioxide for 16h.

Fibroblast-like synoviocytes

Fibroblast-like synoviocytes (FLS) were prepared following established protocols [129]. Briefly, skin was removed from the hind paws of euthanized 6-8 week old mice, the tendons of the ankles were cut, the paws dislodged from the tibias and placed into DMEM containing 1 mg/ml of collagenase IV, 10% FBS and 1% penicillin/streptomycin/glutamine. The joints of the foot were opened using gentle pulling of the foot bones. After a 1-hour incubation at 37°C, the liberated cells were collected, strained though a 70 μm filter (Fisher), and washed with DMEM containing 10% FBS and 1% penicillin/streptomycin/glutamine. The cells were seeded into 10 cm tissue culture coated dishes and cultured at 37°C and 5 % CO_2. Media was exchanged every three days and the cells were passaged using 0.25 % trypsin with 2.21 mM EDTA at near confluency. Cells were used for experiments after three passages. Culture purity was confirmed by flow cytometry analysis using anti-CD90.2, anti-VCAM1 and anti-CD11b antibodies (all from eBioscience). FLS had the spindle-like shape of fibroblasts and were $CD90.2^{+}VCAM1^{+}CD11b^{neg}$.

Microscopy

All images were taken on an EVOS FL Auto (Fisher) and analyzed using the accompanying software.

Quantitative RT-PCR

Total RNA was isolated from cultured cells or pulverized paws using the RNA Easy kit (Qiagen) and cDNA prepared using the QuantiTect kit (Qiagen) according to manufacturer's instructions. Quantitative gene expression for target and housekeeping genes was done using Taqman probes (Applied Biosystems) run on a StepOnePlus Real Time PCR System (Applied Biosystems).

Immunoblotting

Protein extracts were prepared from cultured cells or pulverized paws using RIPA lysis buffer with added protease inhibitors cocktail (Calbiochem), 1 mM phenylmethylsulfonyl fluoride (PMSF, Sigma) and 1 mM sodium orthovanadate (Sigma). Equal numbers of purified human neutrophils and buffy coat cells were directly lysed in SDS-PAGE sample buffer containing

protease inhibitors cocktail, PMSF, sodium orthovanadate and 100 mM dithiothreitol. Equal amounts of protein extract were loaded on TGX Precast gels (Bio-Rad), subjected to SDS-PAGE and transferred onto PVDF membranes using the Trans-Blot Turbo transfer system (Bio-Rad). Immunoblotting was performed using anti-ELMO1 rabbit polyclonal antibody [83], or anti-ERK2, anti-GAPDH or anti-beta-ACTIN-HRP as a loading control. Blots were exposed using the Western Lightning Plus ECL kit (Perkin Elmer) on the ChemiDoc Touch imaging system (Bio-Rad).

Proteomics and Mass Spectrometry

Cells extracts were prepared in Triton X-100 lysis buffer (20 mM Tris, pH 8.0, 137 mM NaCl, 10% glycerol, 0.2% Triton X-100, protease inhibitors cocktail (Calbiochem), 1 mM PMSF and 5 mM sodium orthovanadate) for 1h on ice. Lysates were cleared by centrifugation for 10 min at 13,200 rpm. ELMO1 was immunoprecipitated using the mouse anti-ELMO1 monoclonal antibody [83], and immune complexes were washed and subjected to SDS-PAGE. The gels were stained with SimplyBlue Safe stain (Invitrogen) and destained with water. The gel bands were excised and frozen at -80 °C. After drying in a vacuum centrifuge, the gel bands were digested with 100 µL of trypsin (Promega) (20 µg/mL) at 37 °C for 16 h. The digested peptides were extracted with 100 µL 70% acetonitrile, 5% formic acid in a sonication bath. Each peptide sample was dried in a vacuum centrifuge and resuspended in 16 µL 0.1% TFA. Each gel band digest was analyzed by nanoflow liquid chromatography (LC) (Easy-nLC1000, ThermoFisher Scientific Inc.) coupled online with a an Orbitrap Fusion Lumos Tribrid MS (Thermo Fisher Scientific), samples were loaded on a C18 nano trap column, (Acclaim PepMap100 C18, 2 cm, nanoViper, Thermo Scientific) and resolved on a C18 Easy-Spray column (Acclaim PepMap RSLC C18, 2 µm, 100 Å, 75 µm x 500 mm, nanoViper, Thermo Scientific) with a linear gradient of 2% mobile phase B (95 % acetonitrile with 0.1% formic acid) to 32% mobile phase B within 60 min at a constant flow rate of 250 nL/min. The C18 Easy-Spray column was heated at 50 °C during the analysis. The most intense molecular ions in each MS scan within 3s were sequentially selected for high-energy collisional dissociation (HCD) using a normalized collision energy of 35%. The mass spectra were acquired at the mass range of *m/z* 400-1600. The Easy-Spray ion source (Thermo Scientific) capillary voltage and temperature were set at 1.9 kV and 275 °C, respectively. Dynamic exclusion (30 s) was enabled during the MS/MS data acquisition

to minimize redundant peptide fragmentation events. The RF lens was set to 30% during the MS analysis and both MS1 and MS2 spectra were collected in profile mode. Data was searched against a Swiss-Prot human protein database (http://www.uniprot.org/uniprot/) using Proteome Discoverer (v.2.1.1.21, Thermo Fisher Scientific) via Mascot (v. 2.5.1, Matrix Science Inc.) with the automatic decoy search option set followed by false-discovery rate (FDR) processing by Percolator. Data was searched with a precursor mass tolerance of 10 ppm and a fragment ion tolerance of 0.05 Da, a maximum of two tryptic miscleavages and dynamic modifications for oxidation (15.9949 Da) on methionine residues. Resulting peptide spectral matches (PSMs) were filtered using an FDR of ≤ 1% (Percolator q-value ≤ 0.01). For determination of cell type-specific ELMO1 protein partners, only proteins that were present in all runs were analyzed. We calculated the normalized ratio of the *Elmo1*$^{-/-}$ spectral counts (*Elmo1*$^{-/-}$/*Elmo1*$^{+/+}$+ *Elmo1*$^{-/-}$). This calculation gives a value ranging from 0 to 1 with defined properties, where anything below 0.5 indicates a protein present in *Elmo1*$^{+/+}$ cells but lost in *Elmo1*$^{-/-}$ cells. We considered values at least one standard deviation and 2-fold decreased (e.g. values less than 0.36) to be meaningful ELMO1 binding partners. Cross-comparison of normalized ratios afforded us the ability to then cross-compare ELMO1 binding partners between cell types.

IVIS Imaging

At the indicated time points during K/BxN serum transfer induced arthritis, mice were anesthetized using isoflurane, injected intraperitoneally with 200 µl of 50 mg/ml luminol (Sigma) in sterile saline solution, and scanned/analyzed using the IVIS Spectrum (Perkin Elmer), following manufacturer's instructions.

RNA-Seq analysis

Neutrophils were purified from the bone marrow using anti-Ly6G antibody, as described above. Peritoneal macrophages were prepared as described above. Total RNA was extracted and an mRNA library was prepared using Illumina TruSeq platform and followed by transcriptome sequencing using an Illumina NextSeq 500 cartridge. Cultures from four mice per group were sequenced. The statistical software package R (version 3.3.2) was used for all analyses. The Bioconductor package DESeq2 was used for differential gene expression analysis of RNA-seq data. Heatmaps were created using the R package gplots via the heatmap.2 package. R code used for bioinformatics analysis and heatmap generation is available upon request.

GWAS and experimental linkage analysis

We searched publicly available genome-wide association studies of human disease for SNP by gene interactions. The list of curated databases of published studies that were used is summarized in *Suppl. Table 1*. Significance of a given SNP was determined in the original study. SNP by phenotype interactions were determined using the GWASdb SNP-phenotype association database. The data are plotted using a standardized *p* value as reported [130]. For determination of experimental linkage, a search of curated databases such as the DISEASES experimental gene-disease association database was performed (*Suppl. Table 1*). Significance of the experimental linkage association was determined via a previously established aggregated score [131-135].

Statistical analysis.

Statistical significance was determined using GraphPad Prism 5 or 6 using unpaired Student's two-tailed *t*-test or two-way ANOVA. Variance was similar between groups. No inclusion/exclusion criteria were pre-established. A *p*-value of <0.05 (indicated by one asterisk), <0.01 (indicated by two asterisks), <0.001 (indicated by three asterisks), and <0.0001 (indicated by four asterisks) were considered significant.

Main Figures

Engulfment gene *ELMO1* in neutrophils as a promoter of inflammatory arthritis

Sanja Arandjelovic, Justin S.A. Perry, Christopher D. Lucas, Kristen K. Penberthy, Tae-Hyoun Kim, Ming Zhou, Dorian A Rosen, Tzu-Ying Chuang, Alexandra M. Bettina, Laura S. Shankman, Amanda H. Cohen, Alban Gaultier, Thomas P. Conrads, Minsoo Kim, Michael R. Elliott, and Kodi S. Ravichandran

Fig. 1. Engulfment protein ELMO1 contributes to inflammatory arthritis.

a) Disease SNPs in Rheumatoid Arthritis discovered via search of the GWASdb SNP-disease association database. The data are plotted using a standardized *p* value.

b) Expression of *Elmo1* in total paw extracts from K/BxN mice by qRT-PCR. Each data point represents one mouse.

c, d) ELMO1 protein level by immunoblotting and the quantification in total paw extracts from K/BxN mice and their healthy littermate controls. A representative of two independent experiments is shown. **p<0.01, Student's t-test.

e, f) Schematic of the K/BxN serum induced arthritis model used (e), and immunoblotting for ELMO1 protein in the total paw extracts of *Elmo1*$^{+/+}$ or *Elmo1*$^{-/-}$ mice either day 0 (Control) or day 10 after K/BxN serum injection. Bone marrow derived macrophages (BMDM) are shown as control. A representative of three independent experiments is shown.

g) Paw swelling and clinical scores of *Elmo1*$^{+/+}$ (n=5, white symbols), *Elmo1*$^{+/-}$ (n=7, black symbols) and *Elmo1*$^{-/-}$ (n=5, green symbols) mice injected with 150 µl of K/BxN serum on day 0 and 2. A representative experiment (n=3) is shown. *p<0.05, **p<0.01, ****p<0.0001, Two-way ANOVA.

h) Hind paws of representative mice are shown on day 10 after K/BxN serum injection.

i) H&E staining of hind paws (see Methods) on day10 after K/BxN serum injection. Yellow asterisks indicate areas of inflammatory cell infiltration. Each data point represents one mouse. Scale bar = 1 mm. Data are composite of two independent experiments. ***p<0.001, Student's t-test.

j) Schematic representation of collagen induced arthritis (CIA) induction.

k) Immunoblot analysis of ELMO1 in the total paw extracts from healthy mice or on day 50 after CIA induction. A representative of two independent experiments is shown.

l) Collagen induced arthritis incidence is shown over the indicated time in *Elmo1*$^{+/+}$-DBA (n=13, white symbols), *Elmo1*$^{+/-}$-DBA (n=20, black symbols) and *Elmo1*$^{-/-}$-DBA (n=12, green symbols) mice. Data compiled from three independent experiments is shown.

m) Paw swelling and clinical scores of *Elmo1*$^{+/+}$-DBA (n=13, white symbols), *Elmo1*$^{+/-}$-DBA (n=19, black symbols) and *Elmo1*$^{-/-}$-DBA (n=10, green symbols) mice with CIA. Data from three independent experiments is shown. **p<0.01, ***p<0.001, Two-way ANOVA.

Figure 1. Engulfment protein ELMO1 contributes to inflammatory arthritis.

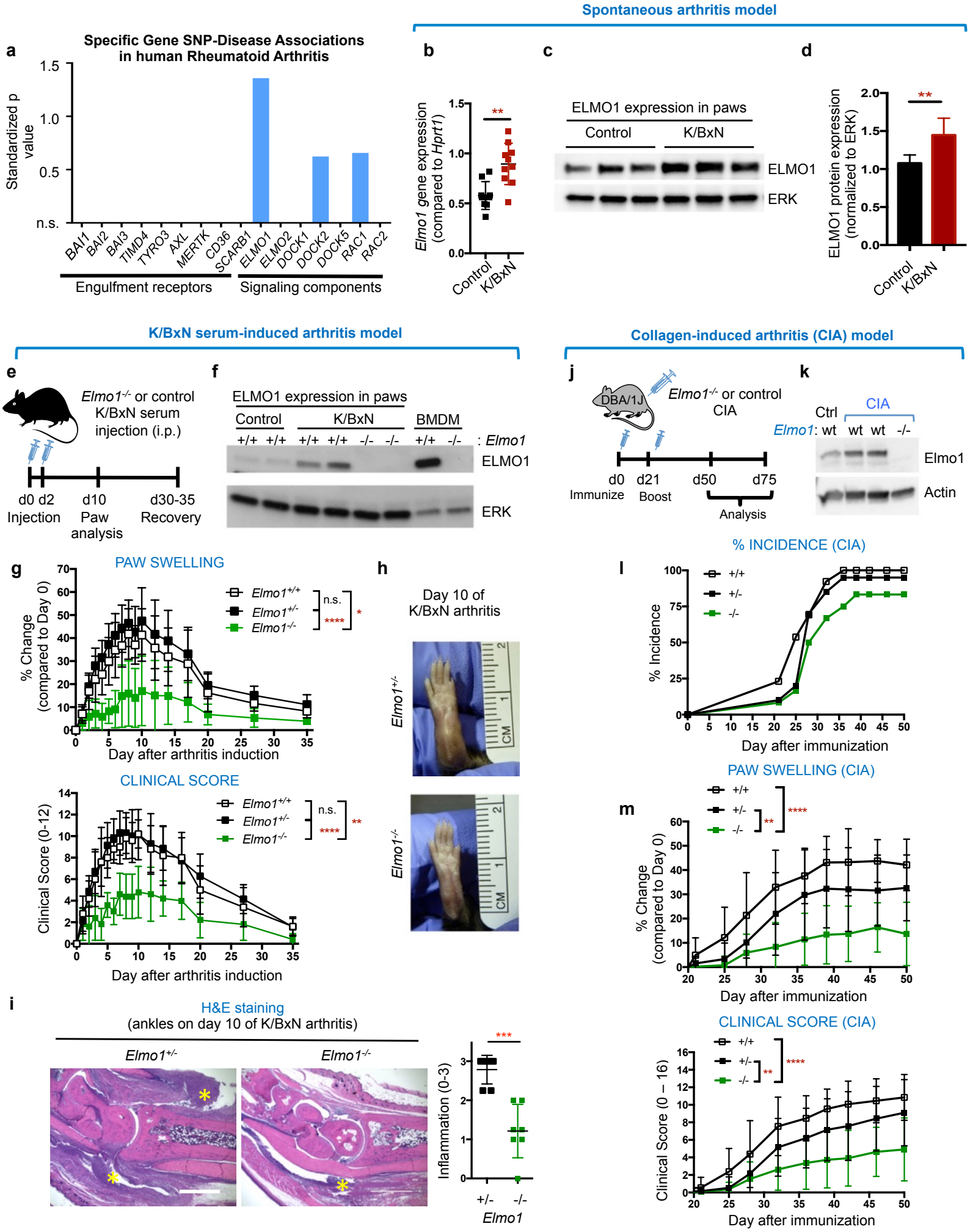

Fig. 2. ELMO1 expression in neutrophils regulates disease severity in arthritis.

a) Hind paw ankle sections were stained with an antibody specific for cleaved caspase-3 (brown) and counter-stained with hematoxylin (blue) on day 10 after K/BxN serum injection. Apoptotic cells are indicated by arrows. Cleaved caspase-3 positive cells were counted in two different fields of view per section, and the average was multiplied by the inflammation score. Each symbol represents an individual animal. **p<0.01, Student's t-test.

b) ELMO1 protein expression in macrophages (left panel) and in purified $Ly6G^+$ bone marrow cells (Neutrophils, right panel). Representative of more than three independent experiments are shown.

c) Paw swelling and clinical scores of female *Elmo1*$^{fl/fl}$ alone or LysM-Cre alone (Control, n=9), or LysM-Cre/*Elmo1*$^{fl/fl}$ (n=9) mice injected with K/BxN serum on day 0 and 2. A composite of three independent experiments is shown. ****p<0.0001, Two-way ANOVA.

d) Representative hind paw ankle sections stained with hematoxylin and eosin on day 10 after K/BxN serum injection. Areas of inflammatory cell infiltration are indicated with yellow asterisks. Scale bar = 1 mm. *p<0.05, Student's t-test.

e) Flow cytometry analysis of paws on day 10 after K/BxN serum injection. Cells in the singlet/$7AAD^{neg}$/$CD45^+$ gate are shown. **p<0.01, Student's t-test.

f) *Elmo1*$^{fl/fl}$ alone and CX3CR1-Cre alone (Control, n=4) or CX3CR1-Cre/*Elmo1*$^{fl/fl}$ (n=4) mice were injected with 150 µl of K/BxN serum on day 0 and 2 and the paw swelling and clinical scores measured as in Fig. 2c.

g) ELMO1 immunoblotting in the resident peritoneal macrophages of indicated mouse strains, as described in the Methods. Representative of three independent experiments is shown.

h) *Elmo1*$^{fl/fl}$ alone and MRP8-Cre alone (Control, n=8) or MRP8-Cre/*Elmo1*$^{fl/fl}$ (n=3) mice were injected with K/BxN serum on day 0 and 2, and the paw swelling and clinical scores measured as in Fig. 2c. A representative of three independent experiments is shown. ***p<0.001, ****p<0.0001, Two-way ANOVA. All data are presented as mean +/- s.d.

i) Representative hind paw ankle sections stained with hematoxylin and eosin on day 10 after K/BxN serum injection. Areas of inflammatory cell infiltration are indicated with yellow asterisks. Scale bar = 1 mm. *p<0.05, Student's t-test.

Figure 2. ELMO1 expression in neutrophils regulates disease severity in arthritis.

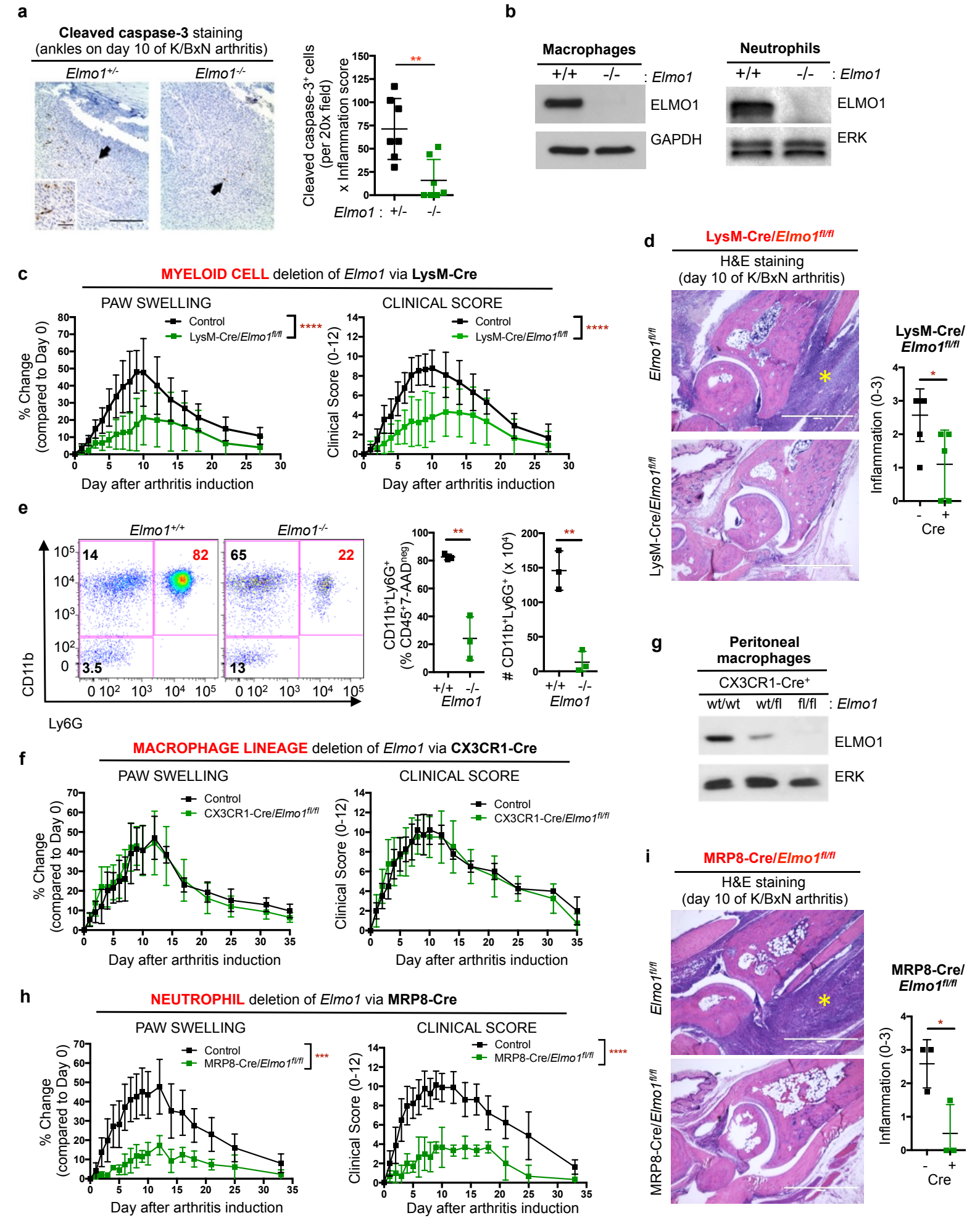

Fig. 3. Neutrophil-specific ELMO1 protein interactome includes regulators of chemotaxis linked to human arthritis.

a) Schematic of the neutrophil and macrophage preparation for proteomic analyses. ELMO1-associated proteins enriched in neutrophils (see *Methods*), when compared to macrophages, are further indicated as neutrophil-specific.

b) Neutrophil-specific ELMO1 protein interaction network analyzed by STRING (string-db.org). Colored nodes indicate query proteins (colors are assigned in arbitrary fashion). Filled nodes represent proteins with known or predicted 3D structure. Known protein interactions are indicated by the magenta (experimentally determined) and cyan (curated database indicated) colored lines. Predicted protein interactions are indicated by green (gene neighborhood), olive (text-mining), black (co-expression) and violet (protein homology) colored lines.

c) Human rheumatoid arthritis associated ELMO1 partners. Among the newly identified neutrophil-specific ELMO1 protein partners, several have known linkages to human arthritis (for references, please see *Results* section). Names of the proteins and genes (between parentheses) are shown. Known biological functions of these proteins and their specific associations with arthritis are listed. RA – rheumatoid arthritis; Tx – therapy.

d) $Ly6G^{+}$ bone marrow cells were purified as described in Methods and cell migration toward LTB4 (1 nM) or CXCL1 (25 ng/ml) was evaluated. A representative of two experiments with two mice per group is shown. *p<0.05, ***p<0.001, Student's t-test.

e) Representative images of migration of $Elmo1^{+/+}$ (n=2) and $Elmo1^{-/-}$ (n=3) neutrophils *in vivo* after laser-induced injury (see Methods). Damaged area is indicated with yellow asterisks. Second harmonic generation (gray), and neutrophils (green) are shown.

f) Track velocity, displacement rate and meandering index of $Elmo1^{+/+}$ (n=2) and $Elmo1^{-/-}$ (n=3) neutrophils before (-) and after (+) laser-induced injury. *p<0.05, **p<0.01, ***p<0.001, ****p<0.0001, Student's t-test.

Figure 3. Neutrophil-specific ELMO1 protein interactome includes regulators of chemotaxis linked to human arthritis.

a

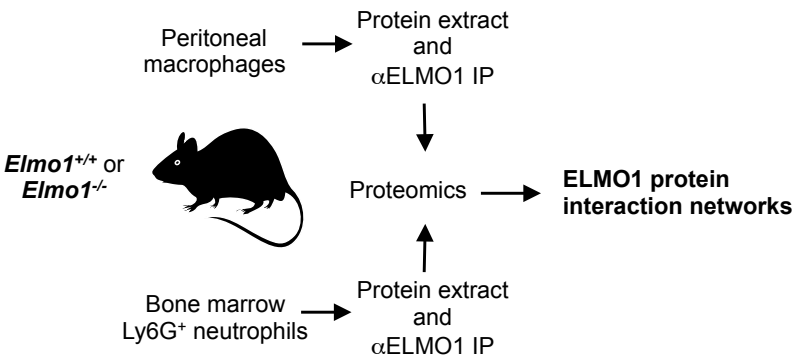

b **Protein-protein interactions between neutrophil-specific ELMO1 partners**

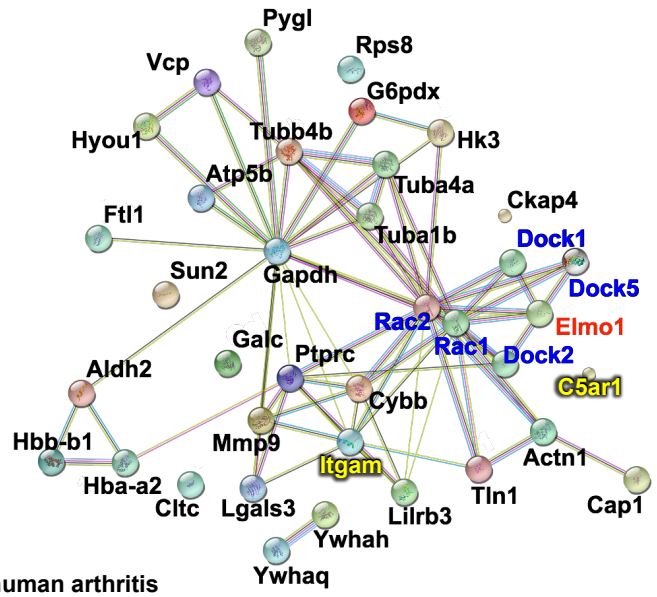

c

Newly identified ELMO1 protein partners in neutrophils with linkage to human arthritis

Protein (Gene)	Function (Reference)	Association with human arthritis (Reference)
CD88 (C5ar1)	Inflammation (62)	Increased levels in RA (72)
CD11b (Itgam)	Cell adhesion (64)	Genetic association (77)
Talin-1 (Tln1)	Actin/cytoskeleton (51, 58)	Proposed biomarker (76)
Alpha-actinin-1 (Actn1)	Actin/cytoskeleton (61)	Increased levels in RA (74)
MMP-9 (Mmp9)	Chemotaxis (53)	Genetic association (70)
Galectin-3 (Lgals3)	Chemotaxis, pleiotropic (54, 56, 63)	Risk allele (73)
CD45 (Ptprc)	Phosphatase (55)	Risk allele, Tx response (69)
14-3-3 protein eta (Ywhah)	Protein-protein interactions (52, 59, 67)	Biomarker, autoantigen (75)
G6PD (G6pdx)	Pentose-Phosphate Pathway (60)	Genetic association (71)
Hexokinase-3 (Hk3)	Glycolysis (66)	Increased levels in RA (68)

d **Purified neutrophil migration**

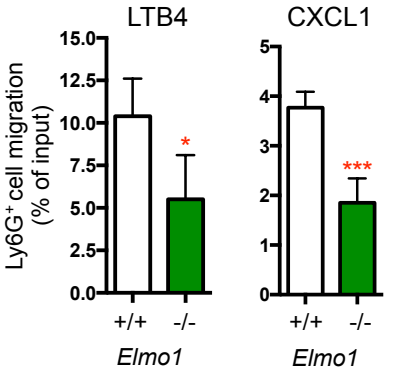

e **Migration of neutrophils** (green) to site of laser induced injury

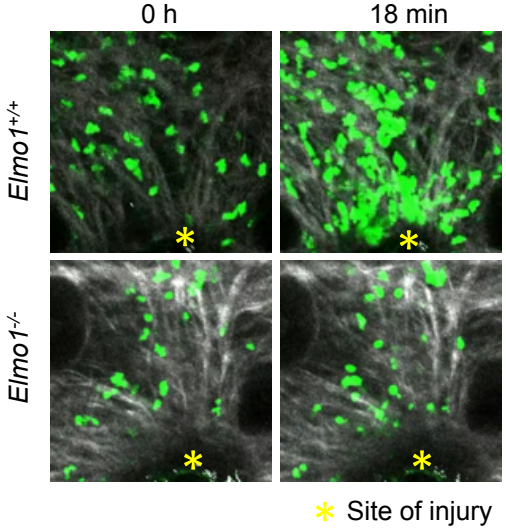

f *In vivo* migration of neutrophils to the site of laser-induced injury

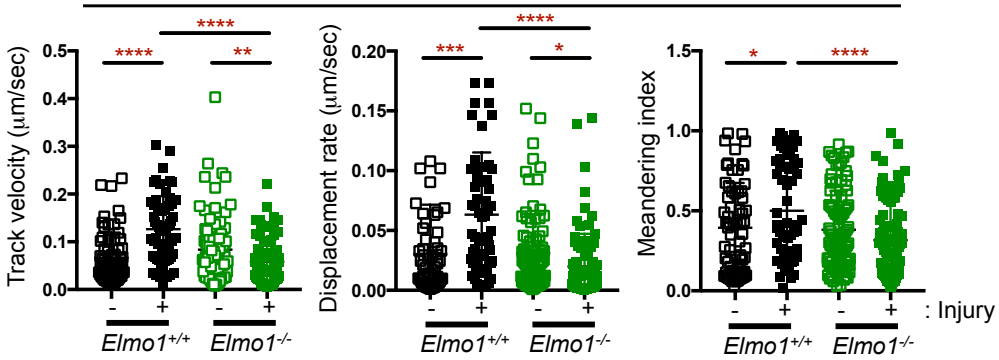

Fig. 4. ELMO1 promotes neutrophil migration to inflamed joints.

a) Mice were injected with luminol on day 1 of K/BxN serum induced arthritis and imaged under anesthesia using the IVIS Spectrum (see Methods). Yellow arrows point to the areas of neutrophil recruitment in the paws. A representative of two independent experiments with two mice per group is shown.

b) Schematic for cell surface CD11b up-regulation upon neutrophil stimulation.

c) Representative flow cytometry of neutrophil cell surface CD11b under resting (Ctrl) conditions or after 1 hour of C5a-, LTB4- or IgG-stimulation.

d) CD11b geometric mean fluorescence index (MFI) in resting (Ctrl) and LTB4- or C5a-stimulated neutrophils purified from *Elmo1*$^{+/+}$ (black, n=4) and *Elmo1*$^{-/-}$ (green, n=4) mice. A representative of six independent experiments with 2-4 mice per group is shown. ****p<0.0001, Student's t-test.

e) C5aR1/CD88 geometric mean fluorescence index (MFI) in resting (Ctrl) and LTB4- or C5a-stimulated neutrophils purified from *Elmo1*$^{+/+}$ (black, n=4) and *Elmo1*$^{-/-}$ (green, n=4) mice (of note, C5a-stimulated C5aR1/CD88 levels were also different from the resting condition with the same level of statistic significance). ****p<0.0001, Student's t-test.

f) Purified neutrophil migration towards LTB4 (1 nM) in the absence (Control, black symbols) or presence of CD11b neutralizing antibody (CD11b Ab, 10 μg/ml, open symbols). Comparison to *Elmo1*$^{-/-}$ neutrophils (green symbols) is shown. The data are composite of two independent experiments and each symbol represents an individual animal. *p<0.05, **p<0.01, Student's t-test.

g) CD11b geometric mean fluorescence index (MFI) in resting (Ctrl) and PMA (50 ng/ml, left panel) or LPS (right panel) stimulated neutrophils purified from *Elmo1*$^{+/+}$ (black, n=3-4) and *Elmo1*$^{-/-}$ (green, n=3) mice.

h) CD11b geometric mean fluorescence index (MFI) in resting (Ctrl) or IgG (plate-bound) stimulated neutrophils purified from *Elmo1*$^{+/+}$ (black) and *Elmo1*$^{-/-}$ (green) mice. A representative of three independent experiments with 2-3 mice per group is shown.

i) Purified neutrophil migration towards supernatants from IgG-stimulated *Elmo1*$^{+/+}$ (black) and *Elmo1*$^{-/-}$ (green) neutrophils. Migration towards LTB4 (10 nM, checkered) was used as a positive

control and vehicle control (Ctrl, white) as a negative control. A representative of three independent experiments with 2-3 mice per stimulation is shown.

j) Schematic of the K/BxN serum transfer arthritis induction and treatment with tamoxifen to induce deletion of *Elmo1* during ongoing arthritis.

k) Clinical scores of male and female Ubc-Cre^{ERt2}/*Elmo1*$^{fl/fl}$ (n=9 for males, n=7 for females, green symbols) and littermate control (n=12 for males, n=10 for females, black symbols) mice with K/BxN serum transfer induced arthritis. Data compiled from three independent experiments is shown. ****p<0.0001, Two-way ANOVA.

l) ELMO1 protein level in the peritoneal (males, top panels) or bone marrow (females, bottom panels) cells from tamoxifen-treated Ubc-Cre^{ERt2}/*Elmo1*$^{fl/fl}$ (+) and littermate control (-) mice with K/BxN serum transfer induced arthritis (day 20 after arthritis induction). All data are presented as mean +/- s.d.

Figure 4. ELMO1 promotes neutrophil migration to inflamed joints.

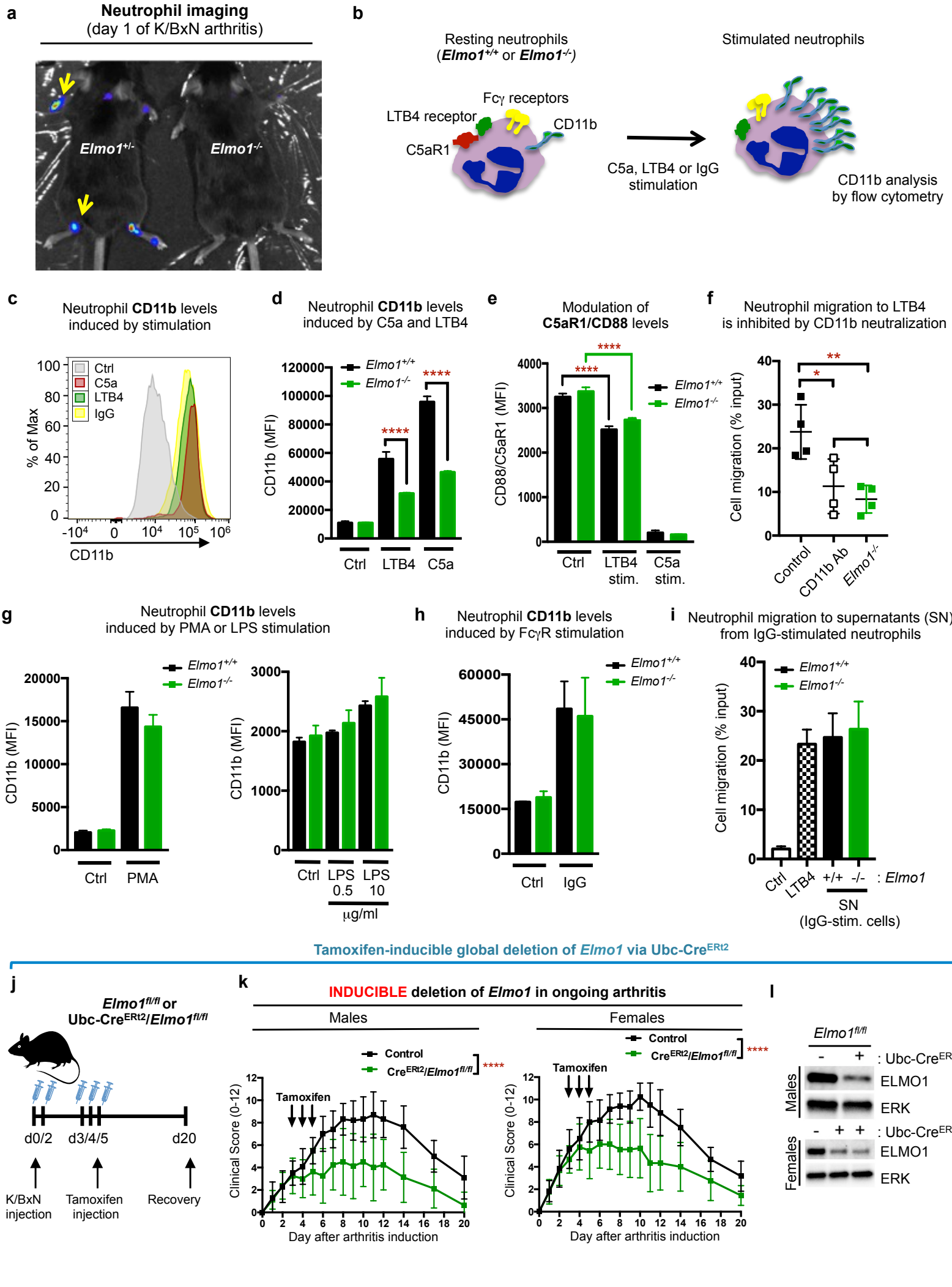

Fig. 5. *Elmo1* function regulates cell type-specific transcriptional programs.

a) Schematic for the preparation of neutrophils and macrophages for RNA isolation and RNA-seq experiments, as described in the Methods.

b) Venn diagram of *Elmo1*-regulated transcripts in neutrophils and macrophages. Examples of shared and cell-type specific *Elmo1*-regulated transcripts are shown. Compared to $Elmo1^{+/+}$ cells, transcripts that are down-regulated in $Elmo1^{-/-}$ cells are indicated in blue text, and transcripts that are up-regulated are shown in red text.

c) Heatmap and list of *Elmo1*-regulated neutrophil-specific transcripts that have associations with human Rheumatoid Arthritis (RA). SNP – single nucleotide polymorphism; Tx – therapy.

d) Quantitative PCR validation of some of the neutrophil-specific arthritis-associated genes in c). Each symbol represents a mouse. All data are presented as mean +/- s.d. *p<0.05, **p<0.01, ****p<0.0001, Student's t-test.

Figure 5. Elmo1 function regulates cell type-specific transcriptional programs.

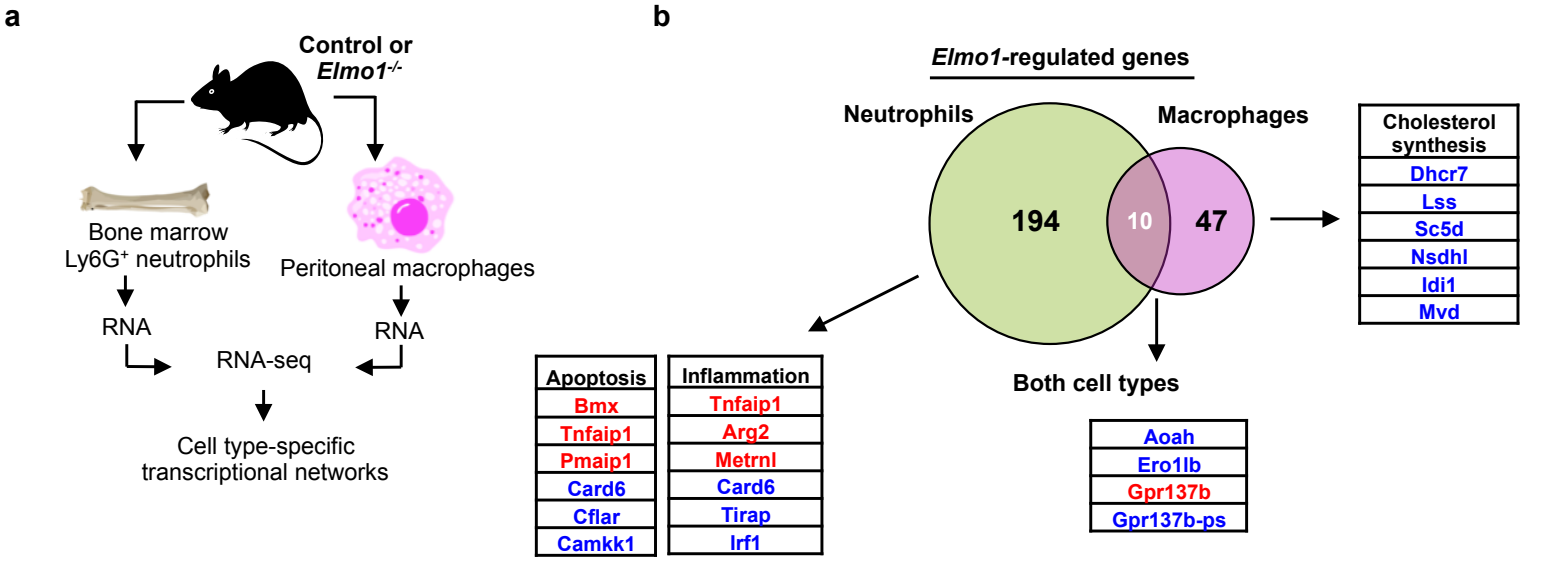

c

Neutrophil-specific genes regulated by *Elmo1* that are linked to rheumatoid arthritis (RA)

Gene	Protein	Fold Change (log_2)	Association with human RA
Cflar	c-FLIP	-0.351	Increased expression, Genetic association, Risk allele, Tx target
Plau	uPA	-0.404	Increased levels in synovial fluid
Rhbdf2	iRHOM2	-0.364	Indirect
Irf1	IRF1	-0.585	Genetic association
Nin	Ninein	-0.329	Autoantigen
Cirbp	CIRBP	0.475	Increased expression, Repressed by TNF-α
Cd84	CD84	0.268	SNP, Tx response
Tnfaip3	A20	0.344	Genetic association, SNP, Decreased expression
Thbs1	TSP1	0.820	Increased plasma levels, Biomarker
Pmaip1	NOXA	0.892	Tx target

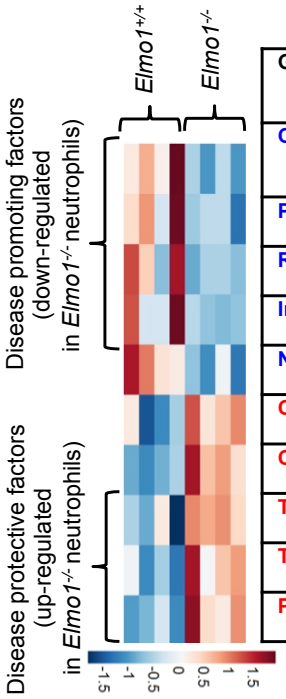

d

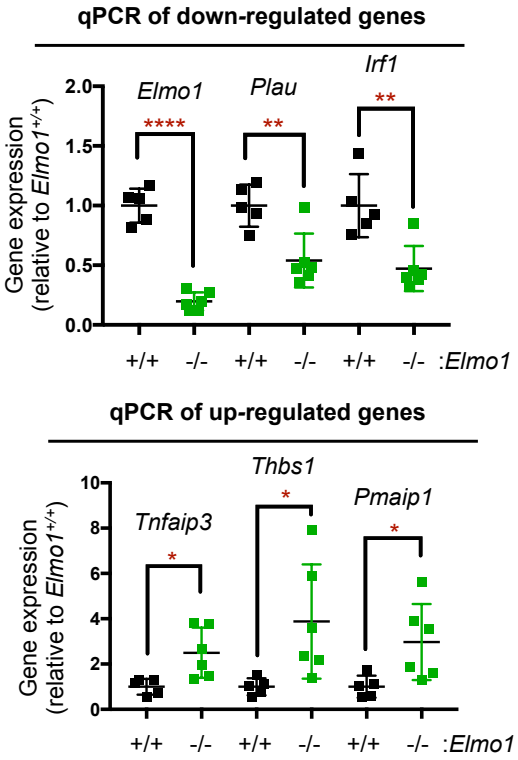

Fig. 6. *ELMO1 rs11984075* SNP promotes migration of human neutrophils.

a) Unique SNPs in *ELMO1* associated with indicated diseases. SNPs are plotted as the negative log of the p value significance by chromosomal position.

b) Allelic discrimination plot of *ELMO1* wild type and rs11984075 SNP alleles in the genomic DNA from healthy human donors in duplicates. Two donors were heterozygous for the *ELMO1* rs11984075 (blue symbols). Two wild type (WT, black symbols) donors are shown. No DNA controls are shown in gray.

c) Immunoblotting of ELMO1 protein expression in peripheral blood neutrophils from human donors homozygous for the *ELMO1* wild type (WT/WT) allele or heterozygous for the *ELMO1* rs11984075 SNP (WT/rs11984075) allele. Protein abundance was normalized to actin levels and presented as fold-WT. Representative of two independent experiments is shown.

d) Transwell migration of purified human peripheral blood neutrophils to LTB4 (15 nM), as described in Methods. Representative of two independent experiments. Data are presented as mean +/- s.d. ***p<0.001, Student's t-test.

e) Representative flow cytometry plot of cell surface L-selectin/CD62L levels on purified human peripheral blood neutrophils from healthy donors without (Control, WT, black line) or with heterozygous *ELMO1* rs11984075 mutation (blue line). FMO, fluorescence minus one. Representative of two independent experiments.

f) Representative flow cytometry plots of CD62L levels on the surface of Ly6G+ peripheral blood neutrophils (left panel) and the quantification of the mean fluorescence index (MFI, right panel). **p<0.01, ***p<0.001, Student's t-test.

g) Representative flow cytometry plots of CD62L levels on the surface of Ly6G+ neutrophils in the bone marrow.

h) ELMO1 protein expression in HL-60 cells stably transfected with non-targeting control (Ctrl) or *ELMO1* targeting shRNA. Actin protein expression is used as a loading control. A representative of three or more independent experiments is shown. A total of three control and four *ELMO1* targeting shRNA single cell clones were analyzed.

i) Migration to LTB4 (100 nM) was evaluated in HL-60 clones expressing control or *ELMO1* targeting shRNA as described in the Methods. A representative of three independent experiments is shown. A total of three control and four *ELMO1* targeting shRNA single cell clones were analyzed. Mean +/- s.d. ***p<0.001, Student's t-test.

Figure 6. Elmo1 function regulates migration in human neutrophils.

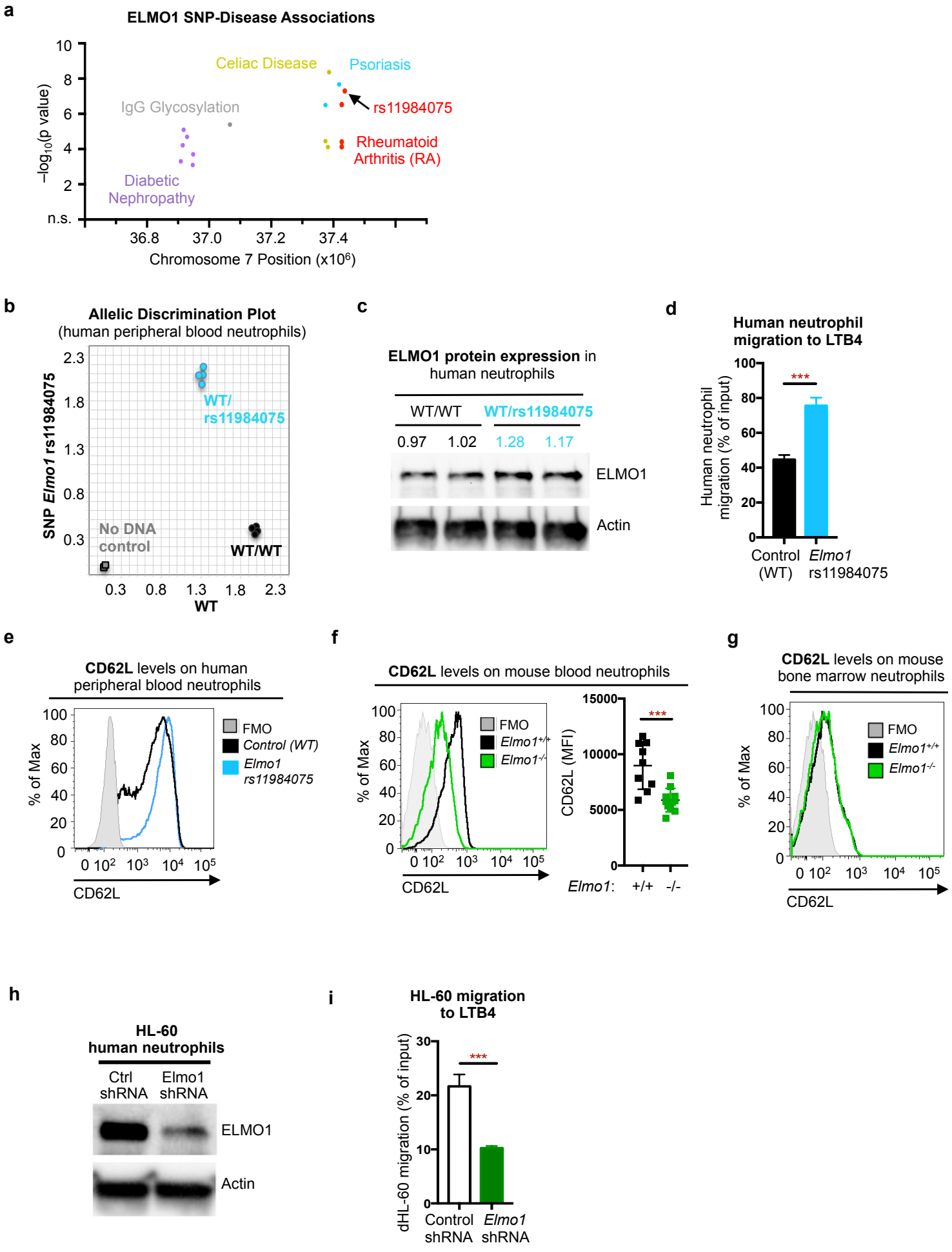

Supplementary Data:

Engulfment gene *ELMO1* in neutrophils as a promoter of inflammatory arthritis

Sanja Arandjelovic, Justin S.A. Perry, Cristopher D. Lucas, Kristen K. Penberthy, Tae-Hyoun Kim, Ming Zhou, Dorian A. Rosen, Tzu-Ying Chuang, Alexandra M. Bettina, Laura S. Shankman, Amanda H. Cohen, Alban Gaultier, Thomas P. Conrads, Minsoo Kim, Michael R. Elliott, and Kodi S. Ravichandran

Supplementary Figure 1. Loss of ELMO1, but not BAI1, reduces disease severity in arthritis.

a) Mice with spontaneous arthritis (K/BxN) or their healthy littermates were used to analyze engulfment machinery expression in isolated paws

b) Expression of apoptotic cell clearance components genes in total paw extracts from K/BxN mice by qRT-PCR. Each data point represents one mouse. *p<0.05, **p<0.01, ***p<0.001, ****p<0.0001, Student's t-test.

c) Incidence of CIA in male *Elmo1*$^{+/+}$-DBA (n=3, white symbols), *Elmo1*$^{+/-}$-DBA (n=12, black symbols) and *Elmo1*$^{-/-}$-DBA (n=5, green symbols).

d) Swelling of the paws was measured (left panel) and clinical scores (right panel) assigned as described in the Methods and are shown for animals presenting clinical signs of disease in c). Data shown are composite of two independent experiments. All data are presented as mean +/- s.d. *p<0.05, Two-way ANOVA.

e) Incidence of CIA in female *Elmo1*$^{+/+}$-DBA (n=5, white symbols), *Elmo1*$^{+/-}$-DBA (n=8, black symbols) and *Elmo1*$^{-/-}$-DBA (n=5, green symbols) (top panel).

f) Swelling of the paws was measured (left panel) and clinical scores (right panel) assigned as described in the Methods and are shown for animals presenting clinical signs of disease in e). Data shown are composite of two independent experiments. All data are presented as mean +/- s.d. *p<0.05, **p<0.01, ***p<0.001, ****p<0.0001, Two-way ANOVA.

g) *Elmo1*, *Elmo2* and *Elmo3* expression was analyzed by quantitative RT-PCR in the total paw extracts of *Elmo1*$^{+/-}$ (black symbols) and *Elmo1*$^{-/-}$ (green symbols) mice on day 10 after K/BxN serum injection. Each symbol represents an individual animal. ***p<0.001, Student's t-test.

h) Schematic of BAI1 binding to ELMO1-DOCK2, leading to the activation of GTPase RAC1.

i) Paw swelling and clinical scores of *BAI1*$^{+/+}$ (n=4, black symbols) and *BAI1*$^{-/-}$ mice (n=11, blue symbols) injected with 150 µl of K/BxN serum on day 0. Data shown are composite of two independent experiments.

Supplementary Figure 1. Loss of ELMO1, but not BAI1, reduces disease severity in arthritis.

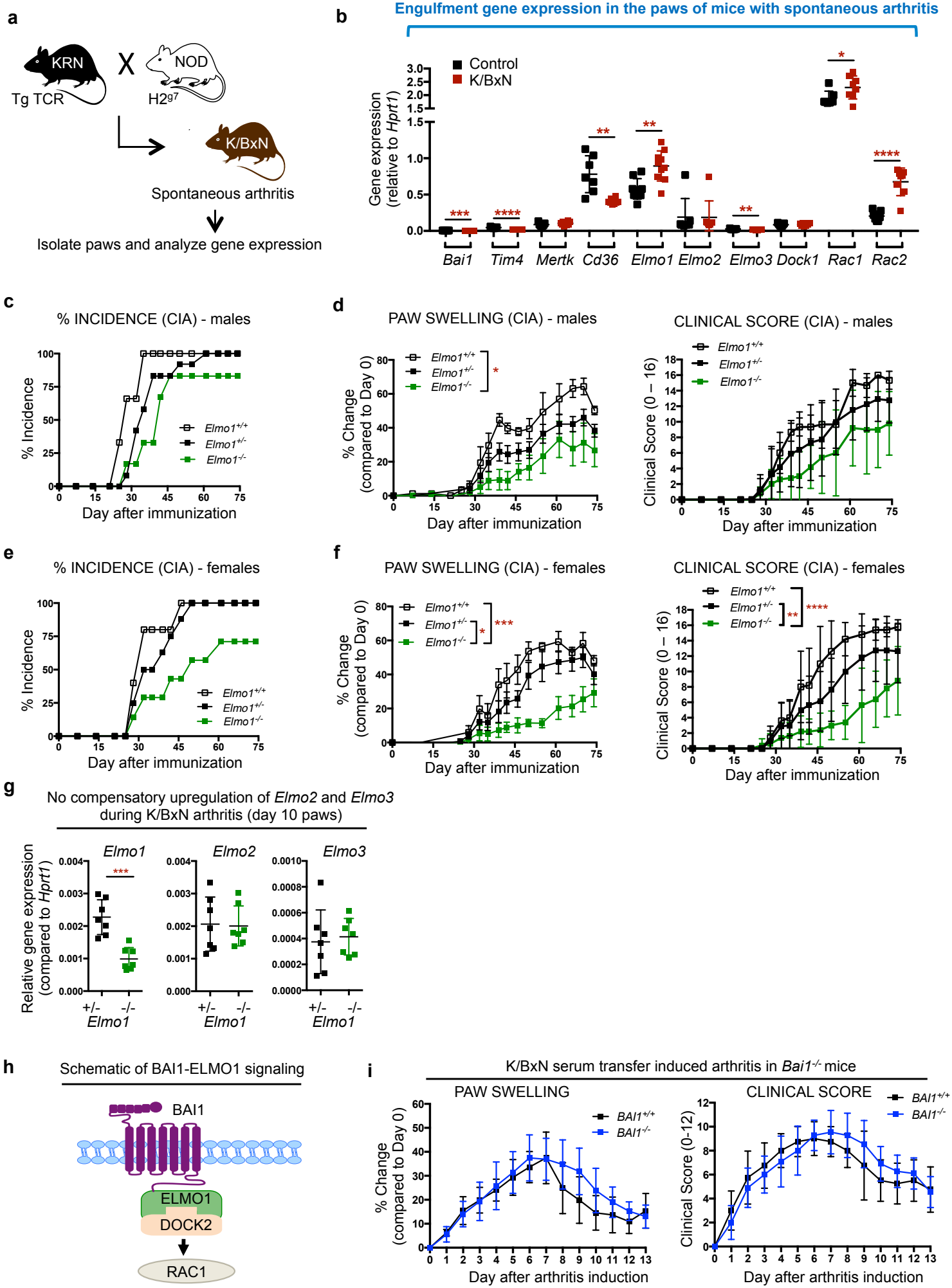

Supplementary Figure 2. ELMO1 expression in neutrophils, but not macrophages, contributes to disease severity in K/BxN serum induced arthritis.

a) Immunoblot analysis of ELMO1 protein expression in resident peritoneal macrophages from indicated mice. A representative of two independent experiments is shown.

b) Paw swelling and clinical scores of wild type (n=4, black symbols) and LysM-Cre (n=3, blue symbols) mice injected with 150 µl of K/BxN serum on day 0 and 2. A representative of two independent experiments is shown.

c) Paw swelling and clinical scores of *Elmo1*$^{fl/fl}$ (Control, n=7) or LysM-Cre/*Elmo1*$^{fl/fl}$ (n=5) mice injected with 150 µl of K/BxN serum on day 0 and 2.

d) Flow cytometry analysis of paws from indicated mice on day 10 after K/BxN serum injection. Cells in the singlet gate are shown.

e) Paw swelling and clinical scores of *Elmo1*$^{fl/fl}$ (Control, n=5) or CX3CR1-Cre/*Elmo1*$^{fl/fl}$ (n=5) mice injected with 150 µl of K/BxN serum on day 0 and 2.

f) Representative hind paw ankle sections stained with hematoxylin and eosin on day 10 after K/BxN serum injection (left panels). Areas of inflammatory cell infiltration are indicated with yellow asterisks. Scale bar = 1 mm. Quantification of inflammation (right panel) indicates no difference between *Elmo1*$^{fl/fl}$ and CX3CR1-Cre/*Elmo1*$^{fl/fl}$ mice.

g) Paw swelling and clinical scores of *Elmo1*$^{fl/fl}$ (Control, n=6) or MRP8-Cre/*Elmo1*$^{fl/fl}$ (n=3) mice injected with 150 µl of K/BxN serum on day 0 and 2.

h) Immunoblot analysis of ELMO1 protein expression in the Ly6G^{+} cells purified from the bone marrow of indicated mouse strains, as described in the Methods. A representative of three independent experiments is shown.

i) Paw swelling and clinical scores of wild type (n=8, black symbols) and MRP8-Cre (n=3, magenta symbols) mice were injected with 150 µl of K/BxN serum on day 0 and 2.

j) Immunoblotting of ELMO1 protein expression in neutrophils purified from the bone marrow and fibroblast like synoviocytes (FLS) from the indicated strains of mice.

Supplementary Figure 2. ELMO1 expression in neutrophils, but not macrophages, contributes to disease severity in K/BxN serum induced arthritis.

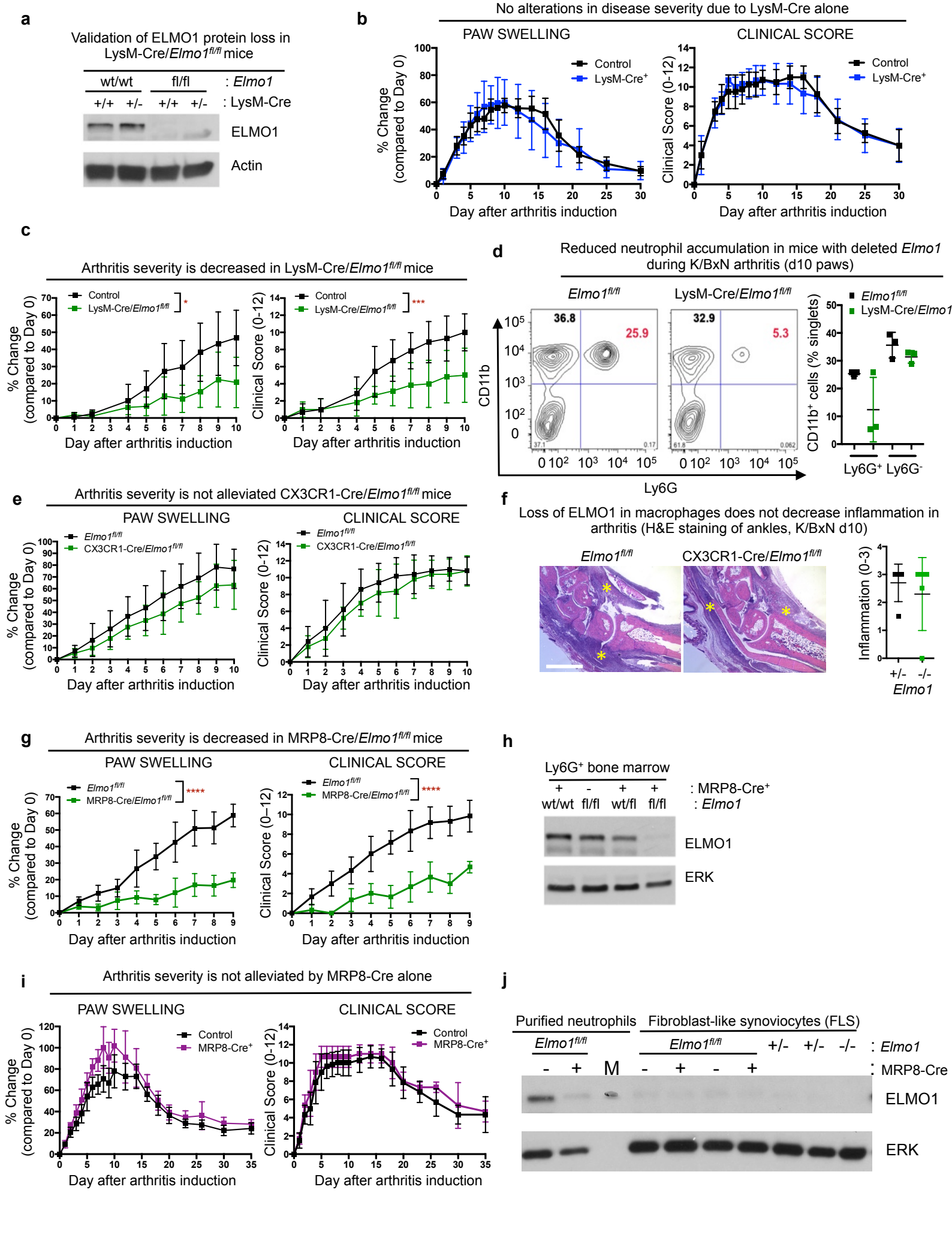

Supplementary Figure 3. Bacterial challenge response and EAE are not changed in *Elmo1*$^{-/-}$ mice.

a) *Elmo1*$^{+/+}$, *Elmo1*$^{-/-}$, *Elmo1*$^{fl/fl}$ and MRP8-Cre/*Elmo1*$^{fl/fl}$ mice were challenged with LPS administered intranasally as described in the Methods and mobilization of neutrophils was analyzed 8 hours later by flow cytometry of cells in the BAL.

b) Quantification of 7-AAD^{-}CD11b^{+}Ly6C^{+}Ly6G^{+} neutrophils in the BAL of mice in a). Each symbol represents an animal. For *Elmo1*$^{+/+}$ and *Elmo1*$^{-/-}$ mice, a representative of two independent experiments is shown.

c) *Elmo1*$^{+/+}$ (n=18) and *Elmo1*$^{-/-}$ (n=19) mice were injected with fecal contents (1.5 mg/g) intraperitoneally to induce fecal-induced peritonitis (FIP) and disease parameters were monitored as described in Methods.

d) Number of Ly6G^{+} neutrophils in the peritoneum 4 hours post FIP induction. Each symbol represents an animal.

e) Temperature of mice in c).

f) Clinical scores of mice in c) were measured as described in Methods.

g) Survival curves of mice in c). All mice alive at 72 hours post FIP induction exhibited complete recovery.

h) Purified neutrophils from *Elmo1*$^{+/+}$ and *Elmo1*$^{-/-}$ mice were incubated with *Klebsiella pneumoniae* at a 1:2 ratio for 1 hour, as described in the Methods, and bacterial killing was analyzed. Each symbol represents neutrophils from an individual animal.

i) *Elmo1*$^{+/-}$ (n=8, black symbols) and *Elmo1*$^{-/-}$ (n=8, green symbols) mice were immunized to induce EAE and disease was scored over the indicated time as described in the Methods. A representative of three independent experiments is shown.

j) Luxol Fast Blue staining of the spinal cords on day 26 after EAE induction (left panel). Demyelination was scored at four different levels of the spinal cord and composite result is shown (right panel). Each symbol represents an individual animal.

Supplementary Figure 3. Bacterial challenge response and EAE are not changed in *Elmo1*$^{-/-}$ mice.

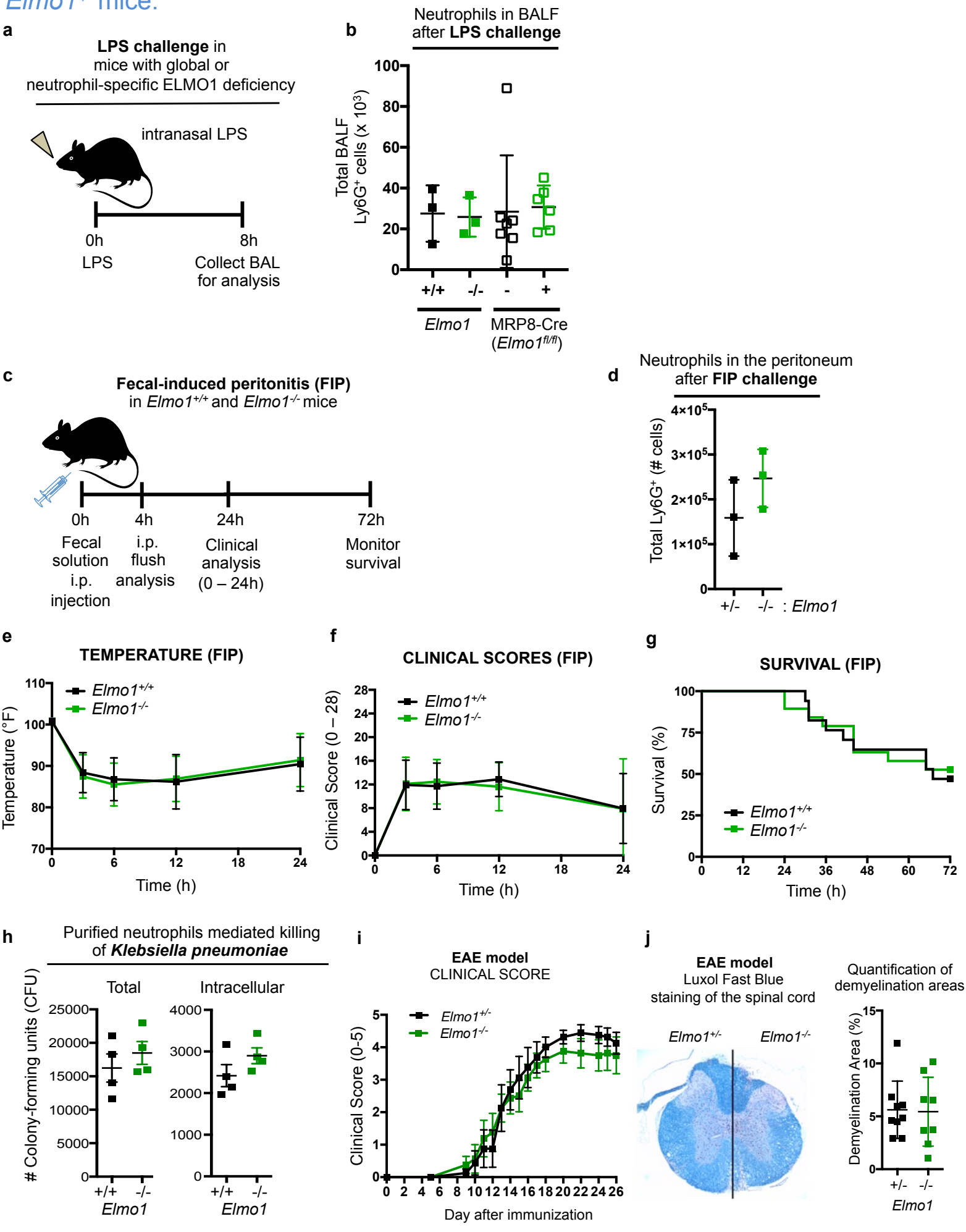

Supplementary Figure 4. *Elmo1* deletion in neutrophils inhibits neutrophil migration.

a) Total bone marrow cells were purified as described in the Methods, and cell migration toward the indicated concentrations of LTB4 or CXCL1 was evaluated after 3 hours at 37°C by flow cytometry. Two mice per group were analyzed. *p<0.05, ***p<0.001, Student's t-test.
b) Transcript levels of the LTB4 receptor *Blt1* are analyzed by qPCR. Representative of two independent experiments.
c) Flow cytometry analysis of cell surface levels of CXCR2 on $Ly6G^+$ neutrophils in the blood (top panels) and the bone marrow (bottom panels) of $Elmo1^{+/+}$ and $Elmo1^{-/-}$ mice. MFI, mean fluorescence index. FMO, fluorescence minus one. Representative of two independent experiments.
d) Flow cytometry analysis of cell surface levels of FcγRIII and FcγRIV on $CD11b^+Ly6G^+$ neutrophils in the blood (top panels) and the bone marrow (bottom panels) of $Elmo1^{+/+}$ and $Elmo1^{-/-}$ mice. Representative of two independent experiments.
e) Immunoblotting of FcγRI protein expression in $Ly6G^+$ neutrophils purified from the bone marrow of $Elmo1^{+/+}$ and $Elmo1^{-/-}$ mice. Representative of two independent experiments.
f) Immunoblotting of Syk protein expression in $Ly6G^+$ neutrophils purified from the bone marrow of $Elmo1^{+/+}$ and $Elmo1^{-/-}$ mice. Representative of two independent experiments.

Supplementary Figure 4. Elmo1 deletion in neutrophils inhibits neutrophil migration.

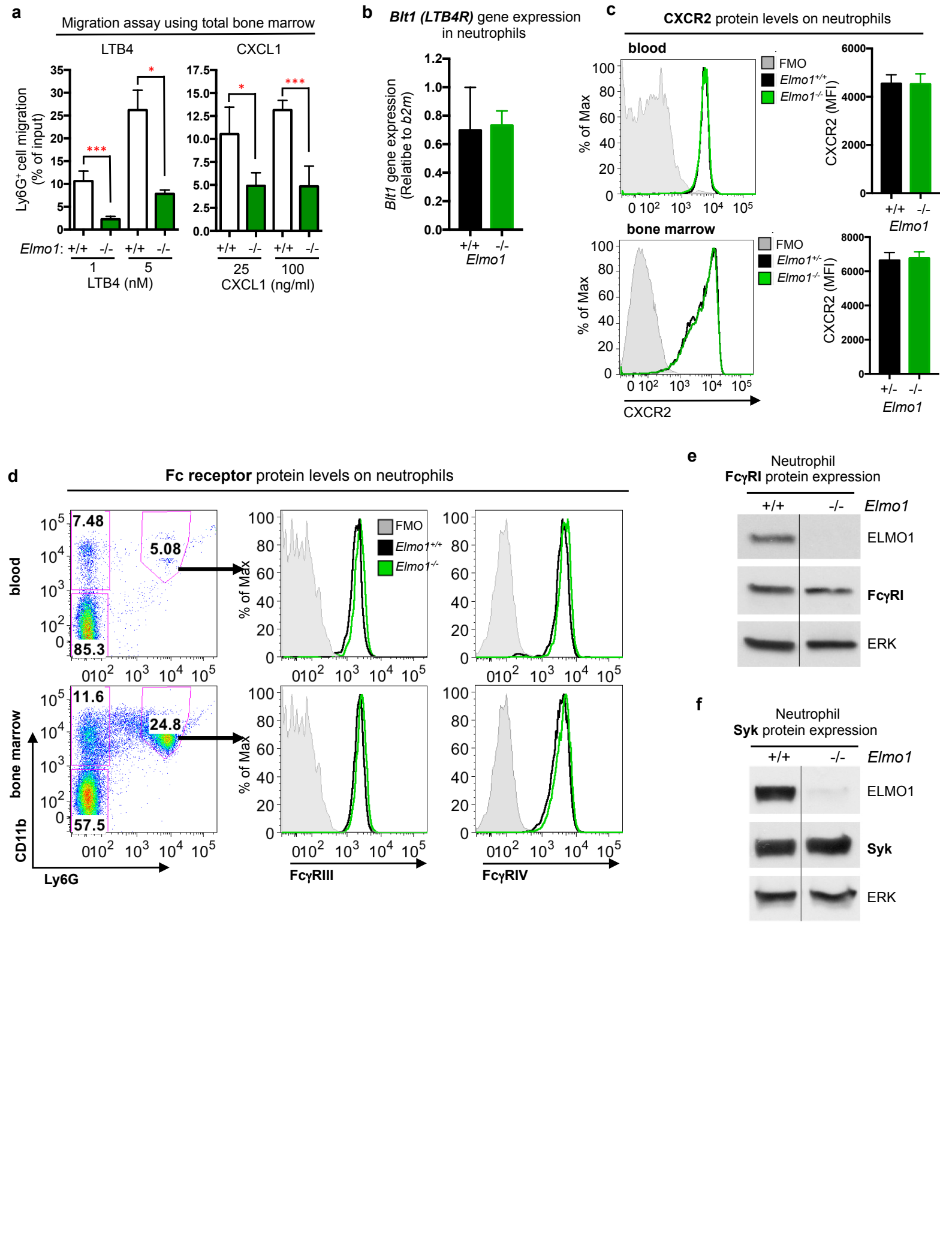

Supplementary Figure 5. Inducible deletion of *Elmo1* in ongoing arthritis.

a) Paw swelling of male and female Ubc-Cre^{ERt2}/*Elmo1*$^{fl/fl}$ (n=9 for males, n=7 for females, green symbols) and littermate control (n=12 for males, n=10 for females, black symbols) mice with K/BxN serum transfer induced arthritis and tamoxifen administration (arrows). Data compiled from three independent experiments is shown. ****p<0.0001, Two-way ANOVA.

b) Paw swelling (left panel) and clinical scores (right panel) of *Elmo1*$^{fl/fl}$ (control, n=5) and Ubc-Cre^{ERt2}/*Elmo1*$^{fl/fl}$ (n=3) mice with K/BxN serum transfer induced arthritis without tamoxifen administration.

c) Schematic of the K/BxN serum transfer arthritis induction and treatment with tamoxifen to induce deletion of *Elmo1* during ongoing arthritis.

d) Paw swelling of male Ubc-Cre^{ERt2}/*Elmo1*$^{fl/fl}$ (n=3, green symbols) and littermate control (n=6, black symbols) mice with K/BxN serum transfer induced arthritis and tamoxifen administration (arrows).

e) ELMO1 protein expression in human peripheral blood neutrophils (duplicates are shown) and buffy coat cells from two different donors (1 and 2). ERK protein expression is used as a loading control. A representative of more than three independent experiments is shown.

Supplementary Figure 5. Inducible deletion of *Elmo1* in ongoing arthritis.

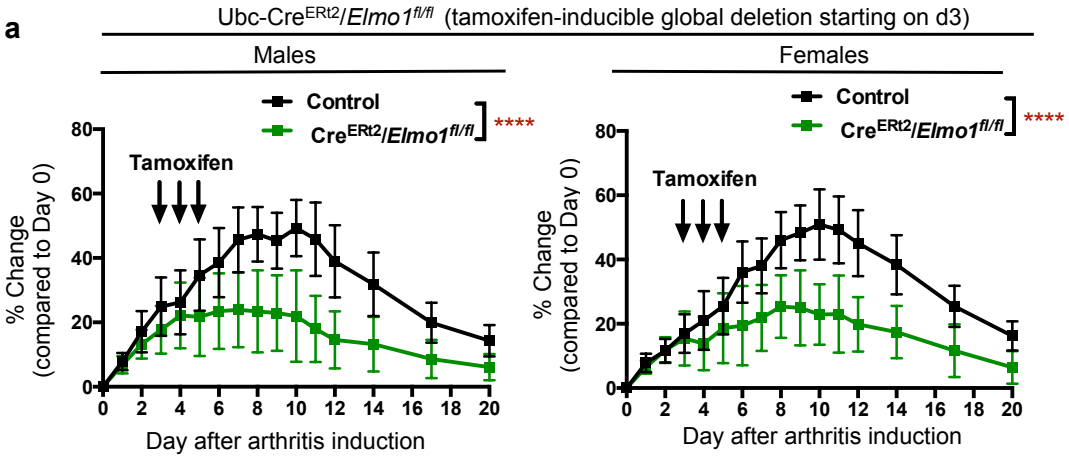

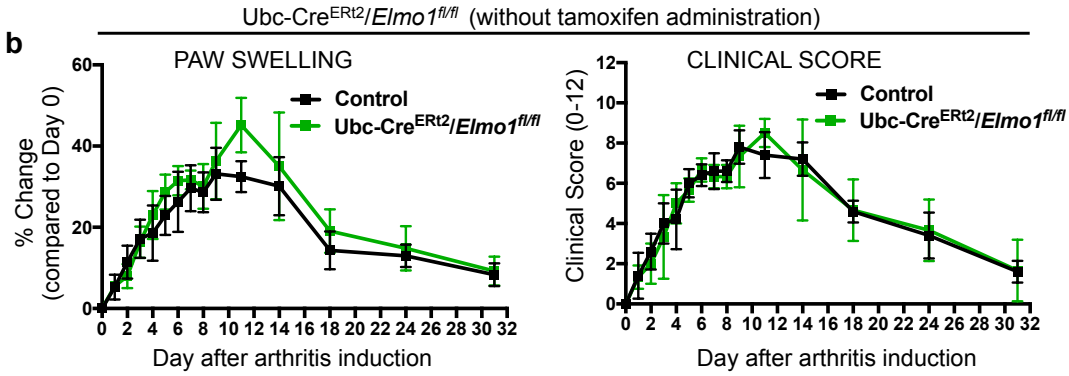

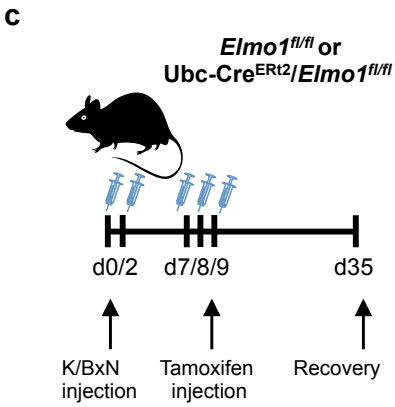

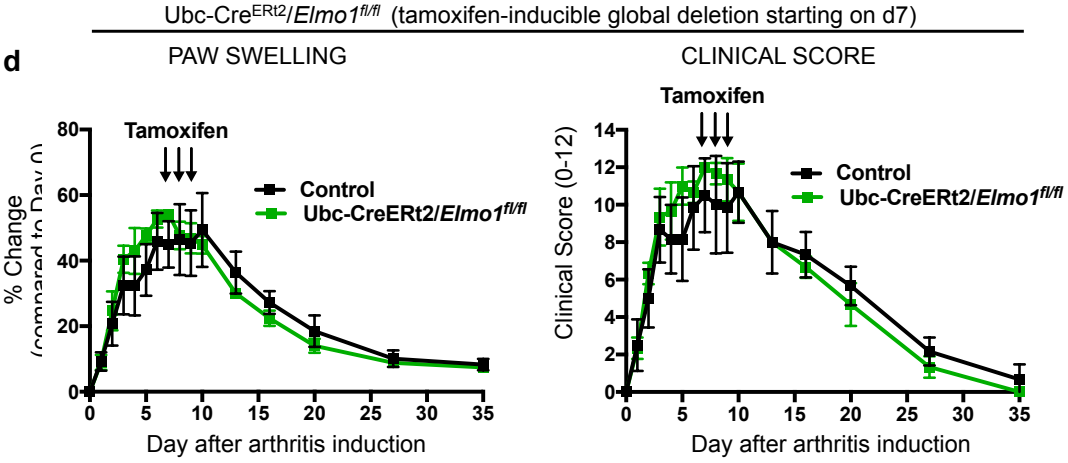

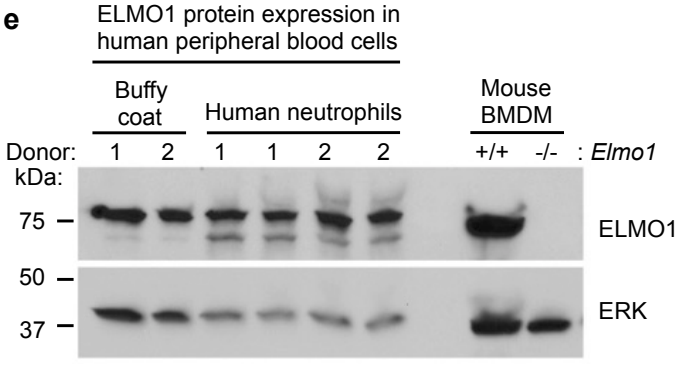

Supplementary Table 1. Details of the databases used and the specific SNPs associated with the indicated genes.

Data Aggregation

Database Name	DOI
GWASdb	10.1093/nar/gkr1182
NHGRI GWAS Catalog	10.1093/nar/gkt1229
Genetic Association Database	10.1038/ng0504-431
GEO Signatures of Differentially Expressed Genes for Diseases	10.1093/nar/gks1193
dbGAP: Database of Genotypes and Phenotypes	10.1093/nar/gkt1211
CTD Gene-Disease Associations	10.1093/nar/gku935
DISEASES Experimental Gene-Disease Assocation Evidence Scores	10.1016/j.ymeth.2014.11.020

SNPs

Gene	Chr	Position	SNP ID	PubMed ID	adj P-value	Population	Trait	SNP Type
Elmo1	7	37436854	rs11984075	21383967	5.00E-08	European(38053)	Celiac & RA	Intron
Elmo1	7	37427351	rs75351767	23143596	2.94E-07	European(27345)	RA	Intron
Elmo1	7	37427351	rs75351767	23143596	3.85E-05	European(27345)	RA (CCP positive)	Intron
Elmo1	7	37427351	rs75351767	23143596	5.95E-05	European(27345)	RA (CCP negative)	Intron
Elmo1	7	37067395	rs10488029	23382691	4.00E-06	European(2247)	IgG glycosylation	Intron
Rac1	7	6434904	rs836472	21452313	1.28E-04	East Asian (1558)	RA	Exon 4
Dock2	5	169461547	rs3763048	23382691	9.00E-06	European(2247)	IgG glycosylation	Intron
Ptprc	1	198640488	rs17668708	24390342	1.70E-05	East Asian(22515), European(57284),ALL(79799)	RA	Intron
Ptprc	1	198640488	rs17668708	24390342	1.80E-05	East Asian(22515)|European(57284)|ALL(79799)	RA	Intron
Ptprc	1	198700442	rs10919563	22446963	3.30E-04	Japanese(20965)|ALL(20965)	RA	Intron
Ptprc	1	198700442	rs10919563	24449572	7.18E-05	European(8305)|ALL(8305)	RA	Intron
Ptprc	1	198700442	rs10919563	23143596	1.25E-10	European(27345)|ALL(27345)	RA	Intron
Lgals3	14	55138318	rs4652	21475983	9.00E-03	Taiwanese(151 RA patients, 182 healthy subjects)	RA	Missense
Cflar	2	201289674	rs6715284	24390342	2.00E-09	58284 European, 22515 East Asian; replication: 9576 European, 13263 East Asian	RA	Intron
Cflar	2	201289674	rs6715284	24390342	3.00E-09	58284 European, 22515 East Asian; replication: 9576 European, 13263 East Asian	RA	Intron
Cd84	1	160513456	rs1503860	23555300	1.38E-07	European(2706)|ALL(2706)	RA, αTNF Tx Response	UTR-3
Cd84	1	160516308	rs6427528	23555300	2.00E-06	European(2706)|ALL(2706)	RA, αTNF Tx Response	UTR-3
Cd84	1	160516308	rs6427528	23555300	7.78E-08	European(2706)|ALL(2706)	RA, αTNF Tx Response	UTR-3
Tnfaip3	6	138195151	rs5029937	22446963	1.40E-07	Japanese(20965)|ALL(20965)	RA	Intron
Tnfaip3	6	138196066	rs2230926	20453841	2.00E-06	Japanese(5683)|ALL(5683)	RA	Missense
Tnfaip3	6	138197506	rs5029949	23143596	3.51E-08	European(27345)|ALL(27345)	RA	Intron
Tnfaip3	6	137685367	rs6920220	17982456	1.00E-07	NOPOP(397), Framingham(1211)	RA	Intron
Tnfaip3	6	137685367	rs6920220	24449572	3.00E-08	European(3223 RA cases, 5,272 controls)	RA	Intron
Tnfaip3	6	137681500	rs10499194	17982456	1.00E-09	NOPOP(397), Framingham(1211)	RA	Intron
Tnfaip3	6	137906227	rs7752903	24390342	7.00E-11	East Asian(22515)|European(57284)|ALL(79799)	RA	Intergenic
Tnfaip3	6	137685367	rs6920220	20453842	9.00E-13	European (5539 patient; 20169 control)	RA	Intron
Tnfaip3	6	137906227	rs7752903	24390342	2.00E-20	East Asian(22515)|European(57284)|ALL(79799)	RA	Intergenic
Tnfaip3	6	137906227	rs7752903	24390342	2.00E-29	East Asian(22515)|European(57284)|ALL(79799)	RA	Intergenic
Tnfaip3	6	138227364	rs7752903	23143596	3.15E-08	European(27345)|ALL(27345)	RA	Intergenic
Tnfaip3	6	138242437	rs6932056	23143596	3.93E-05	European(27345)|ALL(27345)	RA	Intergenic
Tnfaip3	6	138243700	rs61117627	23143596	1.25E-08	European(27345)|ALL(27345)	RA	Intergenic
Tnfaip3	6	138243739	rs58721818	23143596	5.94E-12	European(27345)|ALL(27345)	RA	Intergenic
Tnfaip3	6	138243739	rs58721818	23143596	4.07E-09	European(27345)|ALL(27345)	RA	Intergenic

Supplementary Table 2. Neutrophil-specific ELMO1 protein interactome.

Protein	Gene
Alpha-actinin-1	**Actn1**
Talin-1	**Tln1**
Adenylyl cyclase-associated protein 1	**Cap1**
SUN domain-containing protein 2	**Sun2**
Receptor-type tyrosine-protein phosphatase C	**Ptprc**
ATP synthase subunit beta, mitochondrial	**Atp5b**
Transitional endoplasmic reticulum ATPase	**Vcp**
Glycogen phosphorylase, liver form	**Pygl**
Integrin alpha-M	**Itgam**
Matrix metalloproteinase-9	**Mmp9**
C5a anaphylatoxin chemotactic receptor 1	**C5ar1**
Galectin-3	**Lgals3**
Tubulin beta-4B chain	**Tubb4b**
Tubulin alpha-1B chain	**Tuba1b**
Tubulin alpha-4A chain	**Tuba4a**
Aldehyde dehydrogenase, mitochondrial	**Aldh2**
Galactocerebrosidase	**Galc**
Glyceraldehyde-3-phosphate dehydrogenase	**Gapdh**
Hexokinase-3	**Hk3**
Leukocyte immunoglobulin-like receptor subfamily B member 3	**Lilrb3**
Ferritin light chain 1	**Ftl1**
14-3-3 protein theta	**Ywhaq**
14-3-3 protein eta	**Ywhah**
Hypoxia up-regulated protein 1	**Hyou1**
Hemoglobin subunit beta-1	**Hbb-b1**
Hemoglobin subunit alpha	**Hba**
Glucose-6-phosphate 1-dehydrogenase X (G6PD)	**G6pdx**
40S ribosomal protein S8	**Rps8**
Cytochrome b-245 heavy chain (Nox2, gp91phox)	**Cybb**
Cytoskeleton-associated protein 4	**Ckap4**
Clathrin heavy chain 1	**Cltc**

Suppelementary Table 3. Elmo1 regulates shared and cell type-specific transcriptional programs in neutrophils and macrophages.

Elmo1 regulated genes Fold Change (log2) = Control/*Elmo1* -null

Shared	Fold Change (log2)	
Symbol	Neutrophils	Macrophages
Elmo1	2.88046419	2.355475856
Aoah	0.91585074	0.56933025
Ero1lb	1.37228266	0.852185623
Gpr137b	-1.9799561	-0.927126864
Gpr137b-ps	2.61727206	2.992377917
Hist1h2bc	0.39396578	0.742381795
Zkscan8	-0.5716376	-0.355224675
Stard3nl	-0.3964277	0.430240833
Ggps1	-0.5492517	0.460340538
Hist1h4i	-0.6966969	0.435461088

Neutrophil-specific genes regulated by Elmo1	
Symbol	Fold Change (log2)
Pmaip1	-0.6287105
Dip2c	-0.5581848
Lars2	-0.5143661
Gpr132	-0.4988293
H2-Q7	-0.4852265
H3f3b	-0.4729891
Impact	-0.4575106
Gm23935	-0.4544578
Sertad3	-0.4461594
CT010467.1	-0.43997
H2-Q8	-0.4363432
Thbs1	-0.4180925
Clec7a	-0.4010477
Chrm3	-0.3822215
Mir22hg	-0.3797558
Cirbp	-0.3638295
Wsb1	-0.363417
Btg1	-0.3566311
Slc3a2	-0.3360407
Srgn	-0.3357759
Lgals8	-0.3348986
Dtd1	-0.3347969
Pdcd5	-0.3175303
Frat2	-0.3153359
Pgrmc1	-0.312537
Pik3c3	-0.3072427
Plekha1	-0.3030843
Metrnl	-0.2997594
2410006H16	-0.2961188
Tnfaip3	-0.2948153
Vnn3	-0.2935827
Tspan13	-0.291365
Fundc2	-0.2880764
H2-Q10	-0.2775205
Gm9733	-0.2687127
Eif1	-0.2601325
Cd84	-0.2568044
Tob1	-0.255246
N4bp2l1	-0.2478644
Klra2	-0.2415313
Amica1	-0.2381203
Smim3	-0.2328521
Fcho2	-0.2104856
Vamp3	-0.2098115
Rps14	-0.204736
Slc44a1	-0.1994221
Arg2	-0.1940317
Hgsnat	-0.1929145
Cd24a	-0.182328
Gng2	-0.180254
Smim7	-0.1614396
Dazap2	-0.1429415
Bmx	-0.1189023
Atp8b4	0.16688062
Ankfy1	0.16893629
Ptpn9	0.18710878
N4bp1	0.19170722
Mbnl2	0.19926456
Pfkfb3	0.20030507
Numb	0.20121481
Gabpb2	0.20128893
Ubp1	0.2013883
Elovl1	0.20160334

Macrophage-specific genes regulated by Elmo1	
Symbol	Fold Change (log2)
Il9r	-0.9410805
Igkv9-120	-0.6246305
Cxcl1	-0.5262091
Camk2b	-0.4889724
Igkv4-59	-0.4280269
Ighv8-8	-0.4244122
Ighv14-3	-0.4116772
Ighv10-1	-0.409747
Igkv16-104	-0.3948993
Amigo1	-0.3676841
Phldb1	-0.3651322
Scand1	-0.2930737
Syk	-0.1552282
Mvd	0.15954244
Snx6	0.17639781
Stard4	0.1813722
Sc5d	0.22302841
Twf1	0.22599258
Fgd4	0.2379303
Zak	0.2508524
Dhcr7	0.25397103
Ndufaf7	0.25793667
Nsdhl	0.26838356
Pbx1	0.26915745
Mmab	0.28948315
Hmgcs1	0.30509134
Igkv12-89	0.30760871
Idi1	0.31024232
Lss	0.31529684
Tagap	0.31623132
Fcor	0.40977711
Ifitm6	0.42575208
Lipn	0.44284386
Cfp	0.45686245
Hfe	0.61228442
Akr1c12	0.69589039
Akr1e1	0.79768911

Brd3	0.20470841
Ctr9	0.20633207
Suv420h1	0.21161419
Ncoa3	0.21343811
Atad2b	0.21586325
Stard8	0.21598731
Arhgap27	0.21810428
Ncoa1	0.21994267
Eya3	0.2206874
Clip1	0.22335287
Kidins220	0.22676513
Arhgef11	0.22962916
Myo9b	0.23404124
Tbc1d1	0.23689488
Arid2	0.23731034
Utrn	0.23740368
Myo18a	0.23949916
Tbc1d2	0.24154777
Ncor1	0.24221615
Rbbp6	0.24260904
Arhgef18	0.24380725
Tcf20	0.24806281
Fanca	0.24868013
Jmjd1c	0.25009531
Fkbp5	0.25150588
Upf2	0.25199966
B430306N03	0.25283563
Smarcc2	0.25383235
Aff1	0.25537644
Chdh	0.2574246
Nhsl2	0.25811997
Hcfc1	0.2588155
Tirap	0.25908799
Card6	0.25971648
Rnf24	0.25986769
C2cd3	0.26080834
Ston2	0.26138725
Tnrc18	0.26286031
Usf3	0.2644112
Lhfpl2	0.26698062
Arid1a	0.26721421
Rap1gap2	0.26752142
6430548M08	0.26759788
Mlxip	0.26792125
Tet3	0.26864073
Akna	0.27174232
Pag1	0.27209798
Sipa1l2	0.27230213
Maml1	0.27264292
Cep350	0.27338775
Smarca4	0.27447055
Ccdc88b	0.27520868
Golga3	0.2766627
Bdp1	0.281903
Hivep1	0.28374459
Mrpl49	0.28603615
Myo5a	0.28652454
Sh2b3	0.28660663
Kmt2c	0.28716554
Cdan1	0.28740851
Mkl1	0.28833755
Tnrc6c	0.28957016
Myo1d	0.29027612
Iqsec1	0.29162835
Baz2a	0.29294464
Prrc2a	0.29445331
Nin	0.2958455
Stk10	0.29748554
Fry	0.2995433

Bptf	0.30089401
Rhbdf2	0.30124038
Zmiz1	0.30160412
Anks1	0.30213688
Dhrs9	0.30411591
Trip11	0.30469741
Inhba	0.30602791
A430078G23	0.30692113
Kat6a	0.30775459
Trim16	0.30781937
Yeats2	0.30813637
Dopey2	0.3091297
Golga4	0.31263196
Cflar	0.31271921
Magi3	0.31356419
Kmt2d	0.31465308
Ep300	0.31892093
Ncoa6	0.32318875
Kmt2a	0.3232111
Rrbp1	0.32330835
Cep250	0.32355772
Myh9	0.32534412
Prrc2c	0.326548
Zfp609	0.32962314
Clasp1	0.33104181
Plau	0.33178856
Cdk12	0.3340357
Erc1	0.33440228
Prrc2b	0.33608834
Dcp1a	0.33676443
Ppp1r10	0.33799375
Zfyve26	0.33903101
Setd1b	0.33908818
Tor4a	0.34174994
Golgb1	0.34257573
Rreb1	0.34299995
Kif21b	0.34347578
Plec	0.35394367
Nuak2	0.35804294
Gpr84	0.35936575
Dock5	0.36174605
Ap5b1	0.36196453
Spen	0.36730986
Lmo1	0.36797468
Ankrd11	0.37143906
Camkk1	0.39242286
Rasa2	0.40345356
Bcorl1	0.40379523
Irf1	0.40903726
Ccdc88c	0.43062067
C130026I21R	0.44820577
Zfp142	0.45713544